DOI: 10.1002/ejic.200701130

Alkali Metal (Li^+–Cs^+) Salts with Hexafluorochromate(V), Hexafluorochromate(IV), Pentafluorochromate(IV), and Undecafluorodichromate(IV) Anions

Zoran Mazej*[a] and Evgeny Goreshnik[a]

Keywords: Chromium / Alkali metals / Fluorides / Crystal structures / Hydrogen fluoride

The compounds $ACrF_6$ (A = Li–Cs) were prepared by photochemical reactions of AF/CrF_3 mixtures in anhydrous HF with elemental F_2 at ambient temperature. The crystal structures of compounds $ACrF_6$ (A = K–Cs) are analogous to that of $KOsF_6$, and $NaCrF_6$ exhibits polymorphism. The trigonal phase (II) can be classified to have the well-known $LiSbF_6$ type of structure, while the crystal structure of the orthorhombic modification (I) appears to be a new structure-type. Thermal decomposition of the $ACrF_6$ salts produce $ACrF_5$ (A = Rb, Cs), $ACrF_5/A_2CrF_6$ (A = K), or A_2CrF_6 (A = Li, Na). These compounds undergo partial solvolysis in anhydrous HF with precipitation of CrF_4. From the remaining solutions of the $[CrF_6]^{2-}$ anions and dissolved AF (A = Li–Cs), single crystals of $ACrF_5$ (A = K–Cs), $A_2CrF_6{\cdot}2HF$ (A = Na, K), $A_2CrF_6{\cdot}4HF$ (A = Rb, Cs), Li_2CrF_6, and $K_3Cr_2F_{11}{\cdot}2HF$ were grown, and their crystal structures determined. The main structural feature of the $ACrF_5$ compounds is the infinite zigzag $[CrF_5]_n^{n-}$ chain of distorted $[CrF_6]$ octahedra joined by *cis* vertices. The crystal structures of $A_2CrF_6{\cdot}2HF$ (A = Na, K) and $A_2CrF_6{\cdot}4HF$ (A = Rb, Cs) consist of distorted $[CrF_6]^{2-}$ octahedra involved in moderate to strong hydrogen bonding with HF molecules, while two A^+ cations compensate the negative charge of each octahedron. In $Na_2CrF_6{\cdot}2HF$, two neighboring HF molecules are involved in moderate to strong hydrogen bonding with each other. $(HF)_2$ dimers with a parallelogram structure are formed. The mutual interactions in the crystal structure of $K_2CrF_6{\cdot}2HF$ differ from those found in $Na_2CrF_6{\cdot}2HF$. In the former, each HF molecule interacts with the $[CrF_6]^{2-}$ anion and three K^+ cations. $A_2CrF_6{\cdot}4HF$ compounds of Rb and Cs are isostructural. Their structures consist of A^+ cations and $[CrF_6]^{2-}$ anions involved in hydrogen bonding with two sets of HF molecules in the *trans* position. The crystal structure of $K_3Cr_2F_{11}{\cdot}2HF$ reveals a rare case of the $[M_2F_{11}]^{3-}$ anion.

Introduction

The chemistry of Cr^{5+} and Cr^{4+} is still very limited. Nearly all of the stable Cr^{5+} and Cr^{4+} compounds involve oxygen and/or the halogens.[1–4] They are represented primarily by the black oxochromates(V) of alkali and alkaline earth metals, the red–brown tetraperoxochromates(V), CrO_2, and some peroxo species of Cr^{IV}. Further, there are simple and complex oxohalides such as $CrOF_3$,[5] $CrOCl_3$,[6] $[CrOX_4]^-$ (X = F, Cl, Br) salts,[6,7] and $CrOF_2$.[8] In the case of Cr^{5+} and Cr^{4+} binary and ternary halogenides only the fluoride species are known. Examples of Cr^{5+} compounds are CrF_5[4] and a few $[CrF_6]^-$ salts.[9–11] Chromium(IV) fluorides are represented by CrF_4, which exists in two crystal modifications,[12,13] the very hydrolyzable $[CrF_6]^{2-}$ salts,[6] $ACrF_5$,[14] A_3CrF_7 (A = alkali metal),[15] $XeF_2{\cdot}CrF_4$,[16] $XeF_2{\cdot}2CrF_4$,[17] and $[(XeF_5CrF_5){\cdot}XeF_4]$.[16]

Before this study four $[CrF_6]^-$ salts were known.[10,11] Deep red $NOCrF_6$ was prepared by reaction between NOF and CrF_5 in anhydrous HF (aHF) as solvent.[11] NF_4CrF_6 was obtained after treatment of CrF_5 with excess NF_4HF_2 in aHF solution.[11] NO_2CrF_6 or $CsCrF_6$ were claimed to be prepared by reactions of NO_2F or CsF, respectively, and CrF_5 at elevated temperature.[9] During our work we discovered that previously reported $CsCrF_6$[9] was most likely a mixture of $CsCrF_6$ and Cr^{4+} ternary fluorides. Additionally, $[CrF_6]^-$ salts of Li, Na, K, and Rb were prepared and structurally characterized for the first time. With the exception of the crystal structure of $CrOF_3$,[5] no crystallographic data of other Cr^{5+} compounds could be found in the literature.

Chromium(IV) fluoride complexes of the type $ACrF_5$ (A = K, Rb, Cs) were prepared by reaction of CrF_4 and corresponding alkali metal monofluorides in BrF_3 as solvent, and their lattice constants were reported.[14] By thermal decomposition of the $[CrF_6]^-$ salts, we succeeded in preparing pure $ACrF_5$ compounds. Determination of their crystal structures shows that the previously reported lattice constants were not correct. It should also be mentioned that, with the exception of the recently published crystal

[a] Department of Inorganic Chemistry and Technology, Jožef Stefan Institute,
Jamova 39, 1000 Ljubljana, Slovenia
Fax: +386-1-477-3155
E-mail: zoran.mazej@ijs.si
Supporting information for this article is available on the WWW under http://www.eurjic.org or from the author.

structures of $AZrF_5$,[18,19] $AHfF_5$,[20] and $ATbF_5$,[21,22] no conclusive information was published on the structural arrangements of the $A^IM^{IV}F_5$ (M = transition metal) phases since 1967.[23]

$[CrF_6]^{2-}$ (Li–Cs) salts of alkali metals have been known for a long time. Li_2CrF_6 is formed by fluorination of a $Li_2CO_3/CrCl_3$ reaction mixture at elevated temperature and pressure.[24] The Na–Cs salts could be prepared by fluorination of appropriate mixtures, e.g. KCl and $CrCl_3$,[4,25–27] or by reactions between CrF_4 and AF (A = K–Cs) in BrF_3.[14] There are still some doubts about the purity of those samples because, firstly, losses of Cr (in the form of CrF_5 or oxyfluorides) are inevitable, and secondly, the final products may still contain some BrF_3. During this study we attempted to improve their syntheses and to obtain more information on their crystal structures, since in the literature only lattice constants determined from powder X-ray data are available. Single crystals of Li_2CrF_6 were prepared from HF solution and the crystal structure determined. Instead of yielding the desired A_2CrF_6 compounds, it was found that crystallization from HF solution yielded a completely new set of compounds, which contain HF, i.e. $Na_2CrF_6 \cdot 2HF$, $K_2CrF_6 \cdot 2HF$, and $A_2CrF_6 \cdot 2HF$ (A = Rb, Cs). Additionally, the crystal structure of $K_3Cr_2F_{11} \cdot 2HF$ containing the $[Cr_2F_{11}]^{3-}$ anion (both Cr^{4+}) has been determined. The $[Cr_2F_{11}]^{3-}$ anion, beside the previously known $[Ti_2F_{11}]^{3-}$ anion,[28] is the only example of a dimeric, triply charged anion of transition metals.

Results and Discussion

Syntheses of $ACrF_6$ (A = Li, Na, K, Rb, Cs)

The only previously known alkali metal $[CrF_6]^-$ salt ($CsCrF_6$) was claimed to be prepared by reaction of CsF and CrF_5 at 333 K in a fused silica vessel.[9] It was brick-red and was characterized by infrared spectroscopy (a very strong and very broad band at 600 cm^{-1} and a medium strong band at 295 cm^{-1}). The reported infrared frequencies are in poor agreement with values for other $[CrF_6]^-$ salts.[11] Additionally, the reported brick-red color is typical for $ACr^{IV}F_5$ compounds, while pure $[CrF_6]^-$ salts are deep red (as found in ref.[11] and this work). The reported X-ray powder pattern (neglecting some lines assigned to CrO_3) is more similar to that of $CsCrF_5$ than to that of $KOsF_6$. The majority of AMF_6 compounds whose A^+ cations have radii larger than 1.5 Å crystallize in the $KOsF_6$ structure type (during this study it has been confirmed that this is valid also for $[CrF_6]^-$ salts of K, Rb and Cs).[29] The reported elemental chemical analysis of their product also gave a low value for the fluorine content and a high value for the chromium content.[9] Our attempts to prepare pure $CsCrF_6$ and other $ACrF_6$ (A = Li, Na, K, and Rb) compounds by reactions between the corresponding metal fluoride and CrF_5 at 333 K in reaction vessels made from more inert materials (perfluorinated polymers) than fussed silica failed. In all cases, mixtures of $ACrF_6/A_2CrF_6/ACrF_5$ (A = K, Rb, Cs), $ACrF_6/A_2CrF_6$ (A = Na), or A_2CrF_6 (A = Li) were obtained. Some of the samples still contained unidentified, but most probably polymeric CrF_5, species. The failure of this approach could be attributed to the thermal instability of CrF_5, which starts to decompose at temperatures above 333 K.[16] For that reason, further efforts for the preparation of $[CrF_6]^-$ salts were directed towards the search for low temperature syntheses.

During the last few years, it was found that reactions with UV-irradiated elemental fluorine can be used for the preparation of some ternary fluorides in which the transition metal is in the highest oxidation state by using anhydrous hydrogen fluoride as a solvent.[30–34] The same method was shown to be efficient for the preparation of $ACrF_6$ compounds. In the presence of a UV source, Cr^{3+} is oxidized by fluorine to Cr^{5+} to yield a clear deep-red solution from which pure $ACrF_6$ compounds could be isolated [Equation (1)].

$$AF + CrF_3 + F_2 \xrightarrow[298\ K]{aHF,\ UV} ACrF_6\ (A = Li, Na, K, Rb, Cs) \quad (1)$$

The K, Rb, and Cs salts could be isolated at ambient temperature by pumping away excess fluorine and HF solvent. When $NaCrF_6$ was isolated under the same conditions, the release of CrF_5/F_2 was observed. The dry product consisted of $NaCrF_6$ and a small amount of Na_2CrF_6, and the formation of Na_2CrF_6 could be avoided with isolation at temperatures below 243 K. Dry $NaCrF_6$ is stable at ambient temperature and can be stored in a dry-box. $LiCrF_6$ could be isolated in the same manner, but in contrast to $NaCrF_6$, it immediately started to decopomse at ambient temperature. When fresh aHF was condensed onto freshly isolated $LiCrF_6$ (still cooled below 243 K) and the mixture warmed to ambient temperature, a clear deep-red solution was obtained again. In the Raman spectrum of the solution, only a broad peak around 661 cm^{-1} is observed. This peak could be the corresponding peak of the peak for $CsCrF_6$ dissolved in aHF (659 cm^{-1}), which indicates that in a solution of $LiCrF_6$/aHF, $[CrF_6]^-$ anions are present. When $LiCrF_6$ was warmed up from 243 K to ambient temperature and fresh aHF was condensed onto it, a light-red solid precipitated. The Raman spectrum of the volatiles that were pumped away and caught in liquid nitrogen cooled trap shows the presence of CrF_5, while the remaining residue was Li_2CrF_6. All $[CrF_6]^-$ salts are deep-red, moisture–sensitive, crystalline solids.

Syntheses of $ACrF_5$ and A_2CrF_6 (A = Li, Na, K, Rb, Cs)

As described in the previous paragraph, the thermal stability of the $ACrF_6$ salts increases from Li to Cs, which is in agreement with the general tendency that the thermal stability of $A^IM^VF_6$ compounds increases with increasing ionic radii and with the increasing Lewis basicity of A^+. The final products of the thermal decompostion of the Li and Na salts of $ACrF_6$ are the corresponding A_2CrF_6 salts, while those of the Rb and Cs salts of $ACrF_6$ are the corre-

sponding $ACrF_5$ compounds. The thermal decomposition of $KCrF_6$ lies at the border of the two cases above. When the volatiles were pumped away during the heating of $KCrF_6$, the final product was K_2CrF_6; while $KCrF_5$ was the final product when the decompostion took place in a closed system. By changing the parameters (temperature, pumping), mixtures consisting of different amounts of K_2CrF_6 and $KCrF_5$ were obtained. This could be explained by the following mechanism. First, CrF_5 and fluorine are released, which converts $KCrF_6$ to K_2CrF_6. Chromium pentafluoride starts to decompose to CrF_4 and F_2 at temperatures above 333 K.[16] When CrF_5 is not removed from the system, it decomposes to CrF_4, which further reacts with K_2CrF_6 to finally yield $KCrF_5$. The Rb^+ and Cs^+ ions are weaker Lewis acids than K^+, and their corresponding monofluorides are better fluoride ion donors than KF. Because of this, CrF_5 cannot be released, and $ACrF_6$ is reduced to $ACrF_5$ without the intermediate A_2CrF_6/CrF_4 phase. For Li^+ and Na^+, the opposite occurs. These ions are stronger Lewis acids (i.e. weaker Lewis bases) than K^+, and the corresponding monofluorides are stronger fluoro acids (i.e. poorer fluoro bases or fluoride ion donors) than KF. $LiCrF_6$ and $NaCrF_6$ release CrF_5 and fluorine. When CrF_5 is not removed from the reaction system, it decomposes to CrF_4. The later does not react further with A_2CrF_6 (A = Li, Na) to form the corresponding $ACrF_5$ compounds. The A_2CrF_6/CrF_4 phase is thermodynamically stable in comparison to $ACrF_5$.

Chromium(IV) fluoride complexes of the type $ACrF_5$ (A = K, Rb, Cs) were previously prepared by reaction of CrF_4 and the corresponding alkali metal monofluorides in BrF_3.[14] In the case of K, Rb, and Cs, these reactions were successfully repeated, while attempts to prepare $LiCrF_5$ and $NaCrF_5$ with the same procedure were unsuccessful.

According to literature methods,[25–27] the syntheses of some $[CrF_6]^{2-}$ salts of alkali metals were also checked, i.e. the flow fluorination of a mixture of 2CsCl and $CrCl_3$ at elevated temperature and the reactions between 2AF (A = Na, K, Cs) and CrF_4 in BrF_3. Although the X-ray powder diffraction data of isolated samples corresponded to the literature data, the Raman spectra of the samples show additional bands, which could not be assigned to the $[CrF_6]^{2-}$ salts. An attempt to prepare A_2CrF_6 (A = K, Rb, Cs) by the annealing of $ACrF_5$ and AF or $KF/KCrF_6$ mixtures at elevated temperature were successful for K and Rb but not for Cs. Efforts to purify A_2CrF_6 by crstallization from an HF solution were unsuccessful. A_2CrF_6 and $ACrF_5$ partly solvolyze in contact with fresh aHF to yield an amethyst-colored precipitate (CrF_4) and rose–redd solutions of $[CrF_6]^{2-}$ and dissolved alkali metal monofluorides. In a strongly acidic solvent, HF, the complete solvolysis of $[CrF_6]^{2-}$ is suppressed by the presence of fluoride ions from the dissolved alkali fluorides. With the exception of $[CoF_6]^{2-}$ and $[CuF_6]^{2-}$, the doubly charged $[MF_6]^{2-}$ (M = Ti, Mn, Ni, Pd, etc.) anions are stable in HF. $[MF_6]^{n-}$ (n = 3, 4) anions with a greater negative charge are more basic than $[MF_6]^{2-}$ anions, and more likely to undergo solvolysis in aHF.[35] Crystallization from solutions of $[CrF_6]^{2-}$ and alkali metal monofluorides yielded inhomogeneous products. Single crystals of $A_2CrF_6 \cdot n$HF were found in the powdered material. After HF was released, only a few milligrams of powdered A_2CrF_6 was recovered.

Attempts to Prepare Polyfluorochromates(IV) and -(V)

All attempts to prepare compounds with the anions $[Cr_2F_{11}]^-$, $[Cr_2F_{13}]^{3-}$, or $[Cr_2F_{11}]^{3-}$ (the latter without the presence of HF) failed. Reactions between CrF_3, UV-irradiated F_2, and a corresponding amount of alkali metal fluoride yielded mixtures of $ACrF_6$ (A = alkali metal) and A_2CrF_6 instead of the desired ACr_2F_{11} or $A_3Cr_2F_{13}$.

The annealing of the mixtures $3AF/2CrF_4$, $AF/2ACrF_6$ and $A_2CrF_6/ACrF_6$ always resulted in the A_2CrF_6 compound as the main product instead of the desired $K_3Cr_2F_{11}$. This is in agreement with previous findings of Klemm and Huss.[26] The fluorination of $ACl/CrCl_3$ mixtures in a 3:1 molar ratio at 548 K always resulted in compounds of the type A_2CrF_6.

X-ray Crystal Structures of $ACrF_6$ (A = Na-I, Na-II, K, Rb, Cs)

Single crystals of $ACrF_6$ (A = Na, K, Rb) were prepared by the slow evaporation of volatiles from saturated solutions of the corresponding $ACrF_6$ salts in aHF. For $CsCrF_6$, only the lattice parameters were determined by using the X-ray powder data of $CsCrF_6$ obtained at 298 K, and was indexed by the use of the Dicvol91 program[36] as a trigonal unit cell [a = 7.684(3) Å, c = 7.927(5) Å and V = 405.35 Å^3].

$NaCrF_6$-I and $NaCrF_6$-II

$NaCrF_6$ crystallizes in two different crystal modifications, i.e. as orthorhombic ($NaCrF_6$-I) and trigonal ($NaCrF_6$-II). Both modifications of $NaCrF_6$ are ionic and consist of discrete $[CrF_6]^-$ anions and Na^+ cations that adopt a simple packing arrangement, as depicted in Figures 1 and 2, respectively.

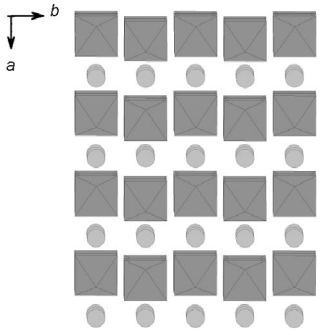

Figure 1. Packing diagram of $NaCrF_6$-I.

The crystal structure of trigonal $NaCrF_6$ (phase-II) is analogous to the well-known $LiSbF_6$ structure.[37] The structure of $LiSbF_6$ is similar to that of VF_3 in terms of

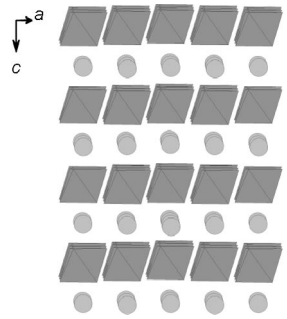

Figure 2. Packing diagram of $NaCrF_6$-II.

cationic ordering. Its structural arrangement can also be described as a rock-salt lattice of Li^+ and $[SbF_6]^-$. Thus, the crystal structure of $NaCrF_6$ is in essence a layer type of structure, which consists of $[CrF_6]^-$ anions and Na^+ cations (Figure 2). Na^+ cations are octahedrally coordinated by fluorine. All Na–F bond lengths are 2.286(5) Å. In the regular $[CrF_6]^-$ octahedra, the six Cr–F distances are 1.722(5) Å.

The orthorhombic crystal structure of $NaCrF_6$ (phase-I) is not related to other AMF_6 structures[29] and appears to be a new type of structure. It consists of Na^+ cations and highly distorted $[CrF_6]^-$ octahedra (Figure 3, Table 2) with Cr–F bond lengths in the range 1.6939(19)–1.8046(13) Å (Table 1). There is a relationship between the Cr–F bond lengths and the corresponding F···Na distances (Figure 3, Table 1): for the longest Cr–F bond (Cr1–F3), the shortest

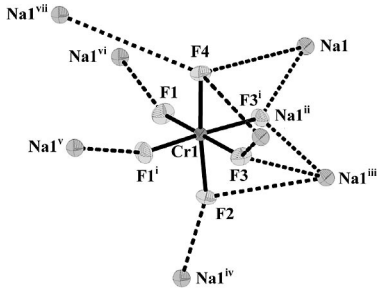

Figure 3. The $[CrF_6]^-$ anion and the closest neighboring Na^+ cations in $NaCrF_6$-I (thermal ellipsoids are drawn at the 50% probability level).

Table 1. Selected Cr–F bond lengths and the corresponding F···Na distances [Å] in $NaCrF_6$-I.[a]

Cr1–F4	1.6939(19)	F4··· Na1	3.626
		F4··· $Na1^{ii}$	3.626
		F4··· $Na1^{vii}$	3.885
Cr1–F2	1.7435(18)	F2···$Na1^{iii}$	3.21
		F2···$Na1^{iv}$	2.398(2)
Cr1–$F1^i$	1.7515(14)	$F1^i$···$Na1^v$	2.3215(16)
Cr1–F1	1.7515(14)	F1···$Na1^{vi}$	2.3215(16)
Cr1–F3	1.8046(13)	F3···$Na1^{ii}$	2.2953(16)
		F3···$Na1^{iii}$	2.5016(18)
Cr1–$F3^i$	1.8046(13)	$F3^i$···Na1	2.2953(16)
		$F3^i$···$Na1^{iii}$	2.5016(18)

[a] Symmetry codes: (i) x, $-y + 1/2$, z; (ii) x, $y - 1$, z; (iii) $-x + 2$, $y - 1/2$, $-z + 1$; (iv) $-x + 3/2$, $-y + 1$, $z - 1/2$; (v) $x - 1/2$, $-y + 1/2$, $-z + 3/2$; (vi) $x - 1/2$, $-y + 3/2$, $-z + 3/2$; (vii) $-x + 3/2$, $-y + 1$, $z + 1/2$.

F···Na contact is found [2.2953(16) Å], and for the shortest Cr–F bond (Cr–F4), the closest Na^+ ions are found at much longer distances (2× 3.626 Å and 3.885 Å).

The Na^+ ions in $NaCrF_6$-II form seven contacts with the fluorine atoms at distances that range from 2.2953(16) Å to 2.5016(18) Å. Bond valence analysis[38–40] around the Na^+ ions arising from these fluorine contacts gives a total bond valence of 1.084 vu (bond valence units).

$KCrF_6$, $RbCrF_6$, and $CsCrF_6$

The crystal structures of $KCrF_6$, $RbCrF_6$, and $CsCrF_6$ are, as expected, analogous to the well-known $KOsF_6$ structure.[29] The $KOsF_6$ structure is found for some KMF_6 compounds and for the majority of AMF_6 compounds whose A^+ cations have a radius larger than 1.5 Å.[29] The structures exhibit nearly regular $[CrF_6]^-$ octahedra with Cr–F bond lengths of 1.750(3) Å (K) and 1.7582(17) Å (Rb). The singly charged cation atoms are coordinated by a total of 12 fluorine atoms [K: 6× 2.833(7) Å and 6× 2.946(4) Å; Rb: 6× 2.9339(18) Å and 6× 3.0708(17) Å].

General Comments on $[CrF_6]^-$ Salts

With the exception of one very short [1.6939(19) Å] and two long [1.8046(13) Å] Cr–F bond lengths in the orthorhombic modification of $NaCrF_6$, all Cr–F bond lengths of $[CrF_6]^-$ salts fall in the same range (1.72 Å–1.76 Å). An average value of 1.743 Å is in excellent agreement with the length of the Cr^{5+}–$F_{terminal}$ bond (1.744 Å) reported for $CrOF_3$.[5] The crystal structure of CrF_5 is not known, and we were not able to find any crystallographic data on other Cr^{5+} fluorides in the literature.

Six-coordinate metal cations with the d^1 electronic configuration (i.e. Cr^{5+}, Mo^{5+}, W^{5+}, Re^{6+}) could be affected by Jahn–Teller distortion.[41] However no distorted structures have been observed so far for compounds with such a configuration. ReF_6 is calculated to be distorted, but experimental proof is still lacking.[41] It is believed that the distortions are all dynamic and are expected to be small. With the exception of the orthorhombic modification of $NaCrF_6$-I, no distortions of the CrF_6 octahedra were observed in the crystal structures of $NaCrF_6$-II, $KCrF_6$, and $RbCrF_6$. In $NaCrF_6$-I, the large distortion in the $[CrF_6]^-$ anion can most likely be attributed to solid-state packing effects.

X-ray Crystal Structures of $ACrF_5$ (A = K, Rb, Cs)

The crystal structures of ternary fluorides of the type $A^IMF^V_5$ are known for some Zr, Hf, Tb, and Te compounds, where Zr^{4+}, Hf^{4+}, and Tb^{4+} are coordinated by eight and Te^{4+} by five fluorine atoms.[18–22] For $KMnF_5$, $KCrF_5$, $RbCrF_5$, and $CsCrF_5$ only lattice constants have previously been reported.[14] However, results for the crystal structure determinations of $KCrF_5$, $RbCrF_5$, and $CsCrF_5$ show that these constants are not correct. $RbCrF_5$ ($KCrF_5$ appears to be isostructural with the Rb compound) and $CsCrF_5$ were found to crystallize in different orthorhombic space groups with four formula units.

The main feature of the $RbCrF_5$ and $CsCrF_5$ structures is an infinite $[CrF_5]_n^{n-}$ chain of distorted $[CrF_6]$ octahedra joined through shared *cis* vertices. The main difference in both structures is the angle of the Cr–F–Cr bridges [Rb: 149.4° (Figure 4); Cs: 180° (Figure 5)]. It appears that this is a consequence of the packing requirements of the smaller Rb^+ cation. This also seems to explain why $LiCrF_5$ and $NaCrF_5$ could not be synthesized, i.e. the interstices in the lattice of the infinite $[CrF_5]_n^{n-}$ chains are too large to be filled by the smaller Li^+ and Na^+ cations. Additionally, because of the high lattice energies of AF, the formation of a mixture of AF/A_2CrF_6 is more preferable than the formation of $ACrF_5$ (A = Li, Na).

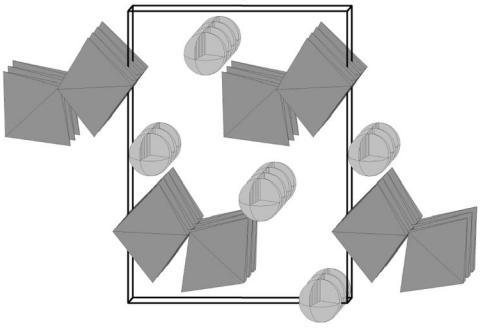

Figure 4. Packing of the infinite $[CrF_5]_n^{n-}$ chains in the crystal structure of $RbCrF_5$ (view along *a* axis).

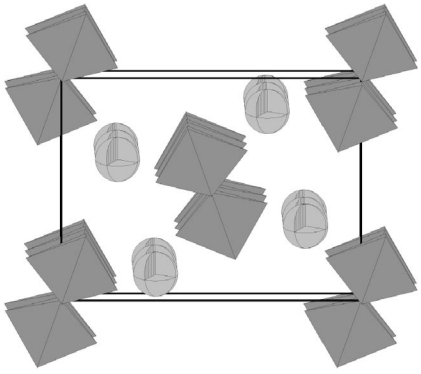

Figure 5. Packing of the infinite $[CrF_5]_n^{n-}$ chains in the crystal structure of $CsCrF_5$ (view along *b* axis).

Although the previously reported lattice parameters of the $ACrF_5$ compounds were in error, the assumption that the $ACrF_5$ complexes consist of $[CrF_6]$ units (rather than isolated $[CrF_5]^-$ anions), each of which share two corners with the neighboring octahedra was correct.[14] The presence of infinite $[CrF_5]_n^{n-}$ chains was previously observed in $XeF_2{\cdot}CrF_4$ ($[CrF_6]$ octahedra share *trans* vertices, Figure 6a),[16] $(XeF_5CrF_5)_4{\cdot}XeF_4$ (alternation of *cis* and *trans* vertices shared between $[CrF_6]$ octahedra, Figure 6b),[16] and XeF_5CrF_5 ($[CrF_6]$ octahedra share *cis* vertices, Figure 6c).[17] The crystal structure of β-CrF_4 also consists of *cis* and *trans* corner-sharing $[CrF_6]$ octahedra, which results in a column-type structure (Figure 6f).[13] In α-CrF_4, columns are formed by $[Cr_2F_{10}]$ dimers (two $[CrF_6]$ octahedra share an edge) that share *trans* vertices.[12] As in XeF_5CrF_5 (Figure 6c), infinite chains of distorted $[CrF_6]$ octahedra joint by shared *cis* vertices are also present in the crystal structures of $RbCrF_5$ and $CsCrF_5$; however, their geometries are different (Figure 6d, e).

Selected bond lengths and angles of $RbCrF_5$ and $CsCrF_5$ are summarized in Tables 2 and 3, respectively, and the structures are shown in Figures 7 and 8, respectively. In $RbCrF_5$ and $CsCrF_5$, distorted $[CrF_6]$ octahedra have four terminal fluorine atoms (F_t) with Cr–F distances in the range 1.743–1.782 Å and two bridging fluorine atoms (F_b) with Cr–F distances of 1.917 Å (Cs) and 1.945 and 1.948 Å (Rb). These values are similar to the Cr–F bond lengths found in $XeF_2{\cdot}CrF_4$ [Cr–F_t:1.71–1.75 Å; Cr–F_b: 1.88 Å],[16] $(XeF_5CrF_5)_4{\cdot}XeF_4$ [Cr–F_t: 1.70–1.716 Å; Cr–F_b: 1.89–1.96 Å],[16] and XeF_5CrF_5 [Cr–F_t: 1.69 Å; Cr–F_b: 1.90 Å–1.97 Å],[17] which are not involved in further contacts with the Xe species.

The *cis* angles in the $[CrF_6]$ octahedra are in the range 82.8–96.3° for the Rb and 84.1–95.6° for the Cs compounds. The Cr–F–Cr bridge in $CsCrF_5$ is symmetric and linear (180°), while in $RbCrF_5$, it is bent with an angle of

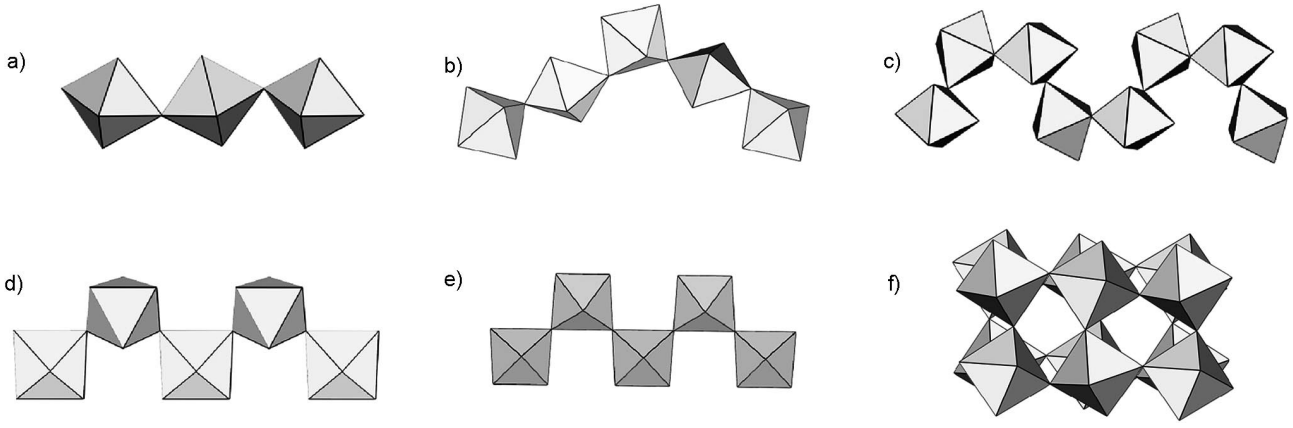

Figure 6. Formation of infinite $[CrF_5]_n^{n-}$ chains in the crystal structures of (a) $XeF_2{\cdot}CrF_4$, (b) $(XeF_5CrF_5){\cdot}XeF_4$, (c) XeF_5CrF_5, (d) $RbCrF_5$, (e) $CsCrF_5$, and (f) β-CrF_4.

Table 2. Selected Cr–F_b bond lengths and Rb···F contacts [Å] and the corresponding bond valences (vu) in $RbCrF_5$.[a]

	Bond length		Bond length	Bond valence		Bond length	Bond valence
Cr1–F11	1.743(8)	Rb2–F22	2.814(8)	0.154	Rb1–F21^{iii}	2.924(6)	0.114
Cr1–F12	1.764(8)	Rb2–F12^{ix}	2.928(3)	0.113	Rb1–F21	2.924(6)	0.114
Cr1–F13^{iii}	1.766(5)	Rb2–F12	2.928(3)	0.113	Rb1–F13^{iv}	3.010(7)	0.09
Cr1–F13	1.766(5)	Rb2–F21^{x}	2.972(7)	0.100	Rb1–F13^{v}	3.010(6)	0.09
Cr1–F1	1.945(5)	Rb2–F21	2.972(7)	0.100	Rb1–F1^{iii}	3.107(6)	0.09
Cr1–F1^{iii}	1.945(5)	Rb2–F13^{xi}	3.010(6)	0.09	Rb1–F1	3.107(6)	0.07
Cr2–F22^{xiv}	1.747(7)	Rb2–F13^{xii}	3.010(6)	0.09			
Cr2–F21^{xv}	1.764(5)	Rb2–F13^{x}	3.185(6)	0.056			
Cr2–F21^{vi}	1.764(5)	Rb2–F13	3.185(6)	0.056			
Cr2–F23	1.782(7)	Rb1–F11^{i}	2.857(8)	0.137			
Cr2–F1	1.948(5)	Rb1–F23	2.891(2)	0.125			
Cr2–F1^{x}	1.948(5)	Rb1–F23^{ii}	2.891(2)	0.125			

[a] Symmetry codes: (i) $-x, -y+1, z-1/2$; (ii) $x-1, y, z$; (iii) $-x, y, z$; (iv) $x, y+1, z$; (v) $-x, y+1, z$; (vi) $x, -y+1, z+1/2$; (vii) $-x, -y+1, z+1/2$; (viii) $x-1, y+1, z$; (ix) $x+1, y, z$; (x) $-x+1, y, z$; (xi) $x, -y, z-1/2$; (xii) $-x+1, -y, z-1/2$; (xiii) $-x, -y, z-1/2$; (xiv) $-x+1, -y, z+1/2$; (xv) $-x+1, -y+1, z+1/2$.

Table 3. Selected bond lengths and Cs···F contacts [Å] and the corresponding bond valences (vu) in $CsCrF_5$.[a]

	Bond length		Bond length	Bond valence		Bond length	Bond valence
Cr1–F1	1.747(6)	Cs1–F2^{i}	3.159(5)	0.097	Cs1–F3^{vi}	3.197(7)	0.088
Cr1–F3	1.757(5)	Cs1–F2^{ii}	3.159(5)	0.097	Cs1–F3	3.197(7)	0.088
Cr1–F3^{x}	1.757(5)	Cs1–F3^{iii}	3.184(6)	0.091	Cs1–F1^{vii}	3.271(7)	0.072
Cr1–F2	1.767(7)	Cs1–F3^{iv}	3.184(6)	0.091	Cs1–F3^{i}	3.291(7)	0.068
Cr1–F4^{xi}	1.917(2)	Cs1–F1	3.188(5)	0.09	Cs1–F3^{viii}	3.291(7)	0.068
Cr1–F4	1.917(2)	Cs1–F1^{v}	3.188(5)	0.09	Cs1–F2^{ix}	3.405(8)	0.05

[a] Symmetry codes: (i) $x-1/2, -y-1/2, -z+3/2$; (ii) $x-1/2, -y+1/2, -z+3/2$; (iii) $-x+1/2, -y, z-1/2$; (iv) $-x+1/2, y-1/2, z-1/2$; (v) $x, y-1, z$; (vi) $x, -y-1/2, z$; (vii) $-x+1/2, y-1/2, z+1/2$; (viii) $x-1/2, y, -z+3/2$; (ix) $-x+1, -y, -z+1$; (x) $x, -y+1/2, z$; (xi) $-x+1, y+1/2, -z+1$.

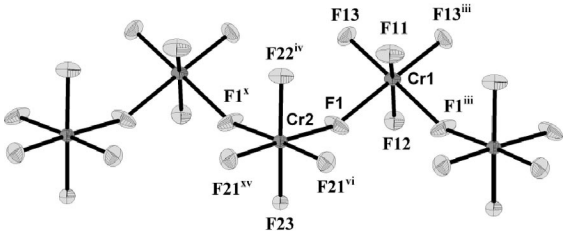

Figure 7. Basic structural unit in $RbCrF_5$; the labeling scheme is shown and the thermal ellipsoids are drawn at the 50% probability level (Rb^+ cations are not shown).

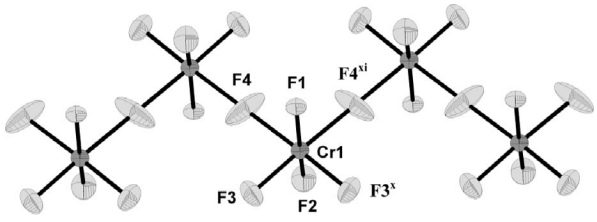

Figure 8. Basic structural unit in $CsCrF_5$; the labeling scheme is shown and the thermal ellipsoids are drawn at the 50% probability level (Cs^+ cations are not shown).

149.4(3)°. It is slightly larger than corresponding angles found in $XeF_2{\cdot}CrF_4$ (147.3°),[16] XeF_5CrF_5 (146.0°),[17] and $(XeF_5CrF_5)_4{\cdot}XeF_4$ (136.6° and 142.3°).[16]

There are two crystallographically independent Rb^+ cations (Rb1 and Rb2) in the crystal structure of $RbCrF_5$. They both form nine Rb···F contacts (Table 2). Athough the total bond valence around both Rb^+ ions arising from these fluorine contacts (Rb2: 2.814–3.185 Å; Rb1: 2.857–3.107 Å) is significantly less than one (Rb1: 0.87 vu; Rb2: 0.94 vu), the next shortest Rb···F distances (Rb2: 2× 3.312 Å and 2× 3.415 Å; Rb1: 2× 3.364 Å and 2× 3.409 Å) could hardly be considered as contacts (the corresponding bond valences are less than 0.05 vu).

The Cs^+ ion in $CsCrF_5$ forms twelve long contacts with distances between 3.159 and 3.405 Å (Table 3). The total bond valence around the Cs^+ ion arising from these fluorine contacts gives a total bond valence of 0.99 vu. The next shortest Cs···F distances (3.747 Å and 3.802 Å) are too long to be considered as contacts (the corresponding bond valences are less than 0.05).

X-ray Crystal Structures of Hexafluorochromates(IV) and $K_3Cr_2F_{11}{\cdot}2HF$

Lattice parameters of hexafluorochromates(IV) with the general formula A_2CrF_6 (Li–Cs) have been known for a long time.[6,14,24,25] They were all determined only from powder X-ray data, and some results were later reinvestigated.[42] Our attempts to prepare single crystals of corresponding $[CrF_6]^{2-}$ salts were successful only in the case of the Li compound. When dissolved in aHF, the compounds A_2CrF_6 and $ACrF_5$ partly solvolyze with the precipitation of CrF_4. From the remaining solution of the $[CrF_6]^{2-}$ anions and dissolved alkali metal fluorides, the single crystals were grown. Two or even more different kinds of crys-

tals were found in the same crystallization batch. In some cases single crystals of the Cr^{IV} compounds were found together with single crystals of the $ACrF_6$ compounds after crystallization of the corresponding $[CrF_6]^-$ salts.

Li_2CrF_6

Li_2CrF_6 was reported previously to be monoclinic (space group $P2_1/c$, a = 4.587 Å, b = 4.584 Å, c = 9.993 Å, β = 117.27°, Z = 2) and isotypic to Na_2SnF_6.[24] The crystal structure of the latter had first been reported to be monoclinic, but later a crystal structure determination of a single crystal showed that it crystallizes with tetragonal symmetry [$P4_2/mnm$, a = 5.0541(4) Å, c = 10.112(3) Å, Z = 2].[43] The results from our study proved that Li_2CrF_6 also does not crystallize in a monoclinic space group, but rather in a tetragonal space group. The crystal structure consists of almost regular $[CrF_6]^{2-}$ octahedra [Cr–F: 4× 1.829(3) Å and 2× 1.812(4) Å] and Li^+ cations. Each Li^+ cation is coordinated by six fluorine atoms [Li–F: 2× 1.996(3) Å, 2× 2.039(9) Å, and 2× 2.054(10) Å].

$Na_2CrF_6{\cdot}2HF$

$Na_2CrF_6{\cdot}2HF$ crystallizes in the monoclinic space group $C2/m$ (No. 14); the unit cell parameters and the crystal and structure refinement data are given in Table 6. Selected bond lengths and angles are summarized in Table 4, and the packing diagram is depicted in Figure 9.

Table 4. Selected Cr–F bond lengths and Na···F contacts [Å] and the corresponding bond valences (vu) in $Na_2CrF_6{\cdot}2HF$.[a]

	Bond length		Bond length	Bond valence
Cr1–F12^{i}	1.7944(16)	Na1–F1	2.349(2)	0.163
Cr1–F12^{ii}	1.7944(16)	Na1–F1^{iv}	2.349(2)	0.163
Cr1–F12^{iii}	1.7944(16)	Na1–F12^{v}	2.3993(19)	0.142
Cr1–F12	1.7944(16)	Na1–F12	2.3993(19)	0.142
Cr1–F11	1.864(2)	Na1–F12^{vi}	2.4070(18)	0.139
Cr1–F11^{iii}	1.864(2)	Na1–F12^{vii}	2.4070(18)	0.139
		Na1–F11^{viii}	2.533(2)	0.099
		Na1–F11^{ix}	2.533(2)	0.099

[a] Symmetry codes: (i) x, $-y$, z; (ii) $-x+2$, y, $-z+2$; (iii) $-x+2$, $-y$, $-z+2$; (iv) $-x+1$, $-y$, $-z+1$; (v) $-x+1$, y, $-z+1$; (vi) $x-1/2$, $-y+1/2$, z; (vii) $-x+3/2$, $-y+1/2$, $-z+1$; (viii) $-x+3/2$, $-y+1/2$, $-z+2$; (ix) $x-1/2$, $y+1/2$, $z-1$; (x) $x+1/2$, $y-1/2$, $z+1$.

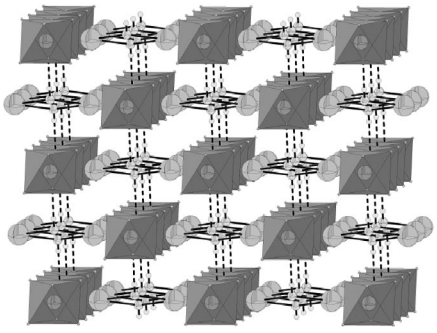

Figure 9. Packing diagram of $Na_2CrF_6{\cdot}2HF$. For reasons of clarity, only Na···F(H) contacts are shown (full lines). Hydrogen bonds are represented by dotted lines.

The structure of the $[CrF_6]^{2-}$ anion and its interactions with the Na^+ cations and HF molecules is given in Figure 10. The basic structural unit is formed by distorted $[CrF_6]^{2-}$ octahedra involved in hydrogen bonding with HF molecules. The *trans* Cr–F11 bonds involved in hydrogen bonding with the HF molecules are significantly elongated [1.864(2) Å] relative to the bond lengths between Cr and terminal fluorine (F12) atoms [4× 1.7944(16) Å]. Hydrogen bonding is further supported by the short F1···F11 distance (2.469 Å).

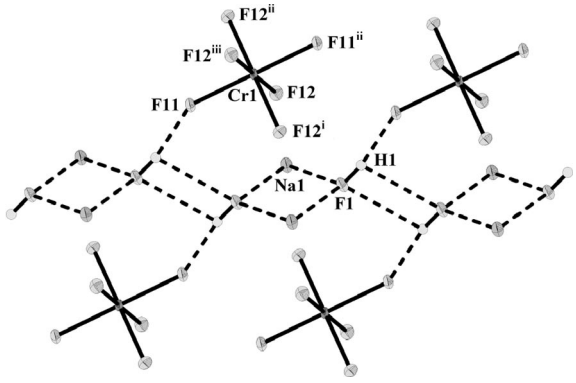

Figure 10. $[CrF_6]^{2-}$ anions and Na^+ cations with interacting HF molecules in $Na_2CrF_6{\cdot}2HF$. For reasons of clarity, only the shortest Na···F contacts are shown. Together with hydrogen bonds, they are presented by dotted lines (thermal ellipsoids are drawn at the 50% probability level).

On the basis of the short distance (2.712 Å) between the fluorine atoms (F1) of two neighboring HF molecules, the HF molecules are also involved in a moderate to strong hydrogen bonding with each other. $(HF)_2$ dimers with a parallelogram structure are formed. In the case of $(HF)_n$ species, only the $(HF)_4$ cluster has been found in the solid phase (in the crystal structure of $[Ir(CO)_6][SbF_6]_3{\cdot}4HF$).[44] Cyclic $(HF)_2$ with a parallelogram and rhombus geometry (the former has a lower energy) has only been examined theoretically as a transition state of the interconversion of two equivalent pseudolinear forms of $(HF)_2$ in the gas phase.[45] The HF···FH distance from theoretical calculations (2.669 Å/2.721 Å)[45] on the cyclic structure with a parallelogram geometry are in excellent agreement with the corresponding distance obtained for the cyclic $(HF)_2$ dimer present in $Na_2CrF_6{\cdot}2HF$. Similar values for internuclear F···F distances were calculated (2.723 Å) and measured [2.72(3) Å] also for the pseudolinear $(HF)_2$ species.[46,47]

The Na^+ cation is coordinated by eight fluorine atoms. Six of them are provided by $[CrF_6]^{2-}$ anions with Na···F contacts in the range 2.3993–2.533 Å (Table 4). The coordination sphere around Na is completed by two fluorine atoms (F1) from HF molecules. The Na···F1 bond lengths are the shortest [2.349(2) Å] among all the Na···F contacts. The total bond valence around both Na^+ ions arising from these fluorine contacts is 1.086 vu (Table 4).

$K_2CrF_6{\cdot}2HF$

The crystal structure of $K_2CrF_6{\cdot}2HF$ also contains $[CrF_6]^{2-}$ anions, singly charged cations (K^+), and neutral

Table 5. Selected Cr–F bond lengths and K···F contacts [Å] and the corresponding bond valences (vu) in K_2CrF_6·2HF.[a]

	Bond length		Bond length	Bond valence		Bond length	Bond valence
Cr1–F12	1.7862(19)	K1–F12^{ii}	2.696(2)	0.150	K1–F13	2.815(2)	0.108
Cr1–F12^{i}	1.7862(19)	K1–F13^{iii}	2.713(2)	0.142	K1–F1^{v}	2.863(3)	0.094
Cr1–F13	1.793(2)	K1–F1	2.750(2)	0.130	K1–F1^{vi}	2.944(2)	0.077
Cr1–F13^{i}	1.793(2)	K1–F12^{iv}	2.767(2)	0.123			
Cr1–F11	1.8814(18)	K1–F11	2.768(2)	0.122			
Cr1–F11^{i}	1.8814(18)	K1–F11^{iv}	2.813(2)	0.109			

[a] Symmetry codes: (i) $-x, -y + 2, -z$; (ii) $-x + 1, -y + 2, -z$; (iii) $-x + 1, y - 1/2, -z + 1/2$; (iv) $x, -y + 3/2, z + 1/2$; (v) $-x + 1, -y + 1, -z$; (vi) $-x + 1, y + 1/2, -z + 1/2$; (vii) $x, y + 1, z$.

HF molecules (Figure 11). However, the interactions of the species in K_2CrF_6·2HF differ from those found in Na_2CrF_6·2HF, and therefore a completely different structure type is obtained. In the latter $(HF)_2$ dimers are present (Figure 10), while in K_2CrF_6·2HF each HF molecule interacts with one $[CrF_6]^{2-}$ anion through F1–H···F11 hydrogen bonding and with three K^+ cations through K···F1–H ionic interactions (Figure 12). All attempts to locate the positions of the hydrogen atoms from Fourier maps were unsuccessful. However, on the basis of the elongation of the two *trans* Cr–F11 bonds (Table 5, Figure 12) and the short F1···F11 contacts (2.455 Å; Figure 12), it was assumed that a hydrogen atom could be placed between F1 and F11 on a calculated position. The F1···F11 contact of 2.455 Å in K_2CrF_6·2HF is similar to the corresponding F1···F11 contact in Na_2CrF_6·2HF (2.469 Å, Figure 10).

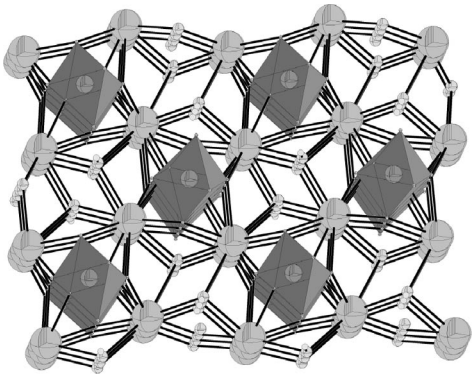

Figure 11. Packing diagram of K_2CrF_6·2HF. For reasons of clarity, the hydrogen bonds are omitted. K···F contacts are shown by full lines (thermal ellipsoids are drawn at the 50% probability level).

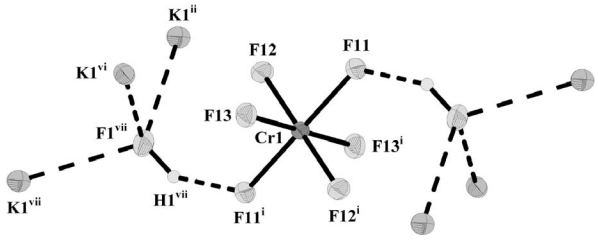

Figure 12. The $[CrF_6]^{2-}$ anion and K^+ cations with interacting HF molecules in K_2CrF_6·2HF (thermal ellipsoids are drawn at the 50% probability level).

Because of the elongated *trans* Cr–F11 bonds and two sets of Cr–F_t bonds [Cr–F12: 2× 1.786(2) Å, Cr–F13: 2× 1.793(2) Å], the $[CrF_6]$ octahedra are not completely regular, although the *cis* F–Cr–F angles are close to 90°.

The K^+ cations are found with an irregular coordination geometry with nine fluorine atoms; K···F contacts are in the range 2.696–2.944 Å (Table 5). The total bond valence around the K^+ ions arising from these fluorine contacts gives a total bond valence of 1.055 vu. For the next shortest K···F distance (3.624 Å), the corresponding bond valence is already less than 0.05.

A_2CrF_6·4HF (A = Rb, Cs)

After crystallization from solutions of partly solvolyzed $ACrF_5$ or A_2CrF_6 (A = Rb, Cs), in addition to light-red crystals of the previously described $ACrF_5$ compounds, yellow–orange crystals were always observed. Attempts to isolate them from the remaining mother liquor at ambient or decreased temperatures always resulted only in a yellow, powdered material corresponding to Rb_2CrF_6 or Cs_2CrF_6, respectively. Later it was found that their decomposition could be suppressed when a small amount of cold perfluorinated oil had been added in the crystallization reaction vessel after crystallization was almost completed. When covered with a thin layer of oil, the yellow–orange crystals do not decompose at temperatures below 273 K and are stable for a few minutes even at ambient temperature. Their single crystal structure analysis explains that phenomenon. During crystallization, single crystals of the compounds with the general formula A_2CrF_6·4HF were grown. During isolation, they release HF to finally yield powdered A_2CrF_6. A thin layer of perfluorinated oil can stop or slow down this process.

Cs_2CrF_6·4HF crystallizes in a monoclinic space group $P2_1/n$ with $Z = 2$. The packing diagram and the basic structural unit with the atom labeling scheme are depicted in Figures 13 and 14, respectively. Selected bond lengths are summarized in Table 6.

As in the case for K_2CrF_6·2HF, all attempts to locate the positions of the hydrogen atoms in Cs_2CrF_6·4HF from Fourier maps failed. However, as was the case for K_2CrF_6·2HF, deformation of the $[CrF_6]$ octahedra {two pairs of elongated *trans* Cr–F bonds [Cr–F11: 2× 1.818(8) Å, Cr–F13: 2× 1.849(8) Å] and one pair of shorter *trans* Cr–F12 bonds [2× 1.784(7) Å], together with short F2···F11 and F1···F13 distances (2.462 Å and 2.472 Å;

Table 6. Selected Cr–F bond lengths and Cs···F contacts [Å] and the corresponding bond valences (vu) in Cs_2CrF_6·4HF.[a]

	Bond length		Bond length	Bond valence		Bond length	Bond valence
Cr1–F12^{ii}	1.784(7)	Cs1–F12^{i}	3.089(8)	0.118	Cs1–F13^{iv}	3.175(8)	0.093
Cr1–F12	1.784(7)	Cs1–F11^{ii}	3.120(9)	0.108	Cs1–F2^{v}	3.213(10)	0.084
Cr1–F11	1.818(8)	Cs1–F12	3.159(8)	0.097	Cs1–F1^{vi}	3.297(9)	0.067
Cr1–F11^{ii}	1.818(8)	Cs1–F12^{iii}	3.162(7)	0.097	Cs1–F1^{vii}	3.302(8)	0.066
Cr1–F13^{ii}	1.849(8)	Cs1–F1	3.166(10)	0.096	Cs1–F2^{iii}	3.332(9)	0.061
Cr1–F13	1.849(8)	Cs1–F2	3.173(9)	0.094	Cs1–F13	3.451(9)	0.044

[a] Symmetry codes: (i) $x + 1/2, -y + 3/2, z + 1/2$; (ii) $-x + 2, -y + 2, -z$; (iii) $-x + 3/2, y - 1/2, -z + 1/2$; (iv) $-x + 5/2, y - 1/2, -z + 1/2$; (v) $-x + 2, -y + 2, -z + 1$; (vi) $-x + 2, -y + 1, -z + 1$; (vii) $-x + 3/2, y + 1/2, -z + 1/2$; (viii) $x, y + 1, z$; (ix) $x - 1/2, 5/2 - y, z - 1/2$.

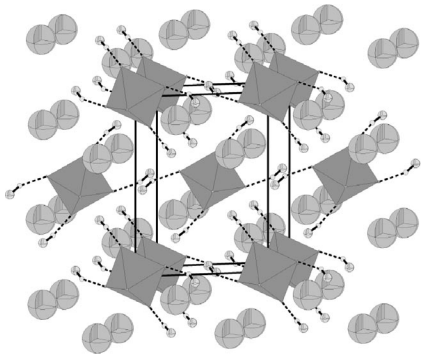

Figure 13. Packing diagram of Cs_2CrF_6·4HF. For reasons of clarity, Cs–F contacts are not shown. Hydrogen bonds are presented by dotted lines (thermal ellipsoids are drawn at the 50% probability level).

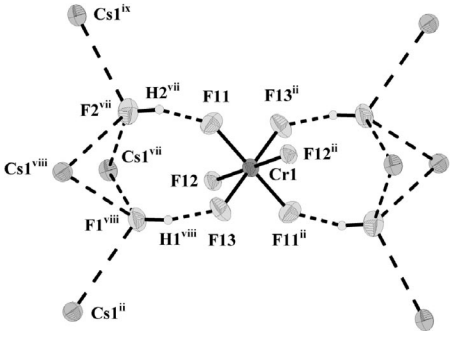

Figure 14. The $[CrF_6]^{2-}$ anion and Cs^+ cations with interacting HF molecules in Cs_2CrF_6·4HF (thermal ellipsoids are drawn at the 50% probability level).

Figure 13)} indicates that hydrogen atoms could be placed between F1 and F13 (F2 and F11) on calculated positions.

Taking the coordination number to be defined as the number of nearest neighboring atoms, then Cs^+ is surrounded by 12 fluorine atoms at distances between 3.089(8) and 3.451(9) Å (Table 9). The total bond valence around Cs^+ is 1.025 vu (Table 6).

$K_3Cr_2F_{11}$·2HF

There are many reports on crystal structures of compounds with the general formula $A^IB^{II}Zr_2F_{11}$ (A = alkali metal, B = transition metal) and LnM_2F_{11} (Ln = rare earth metal, M = Zr^{4+}, Hf^{4+}, Th^{4+}).[48–50] Isolated $[M_2F_{11}]^{3-}$ anions are not reported in any of these papers. $[C_5H_6]_2[H_3O][Ti_2F_{11}]$·$2H_2O$ is the only compound for which the isolated triply charged dimeric anion ($[Ti_2F_{11}]^{3-}$) was found in the crystal structure.[28] The crystal structure of $K_3Cr_2F_{11}$·2HF represents the second example with the $[M_2F_{11}]^{3-}$ anion (Figure 15).

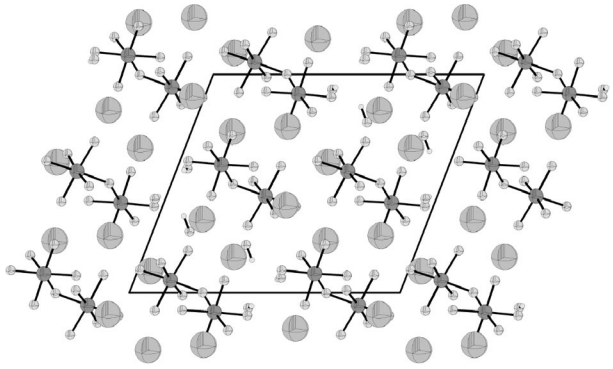

Figure 15. Packing diagram of $K_3Cr_2F_{11}$·2HF.

The crystal structure of $K_3Cr_2F_{11}$·2HF reveals that the $[M_2F_{11}]^{3-}$ anions are highly distorted from the ideal D_{4h} symmetry (Figure 16) and that there are three crystallographically nonequivalent K atoms and two crystallographically nonequivalent HF molecules. Distortions of the $[M_2F_{11}]$ units are usually expressed in terms of the bridging angle α (bending of $F_5M–F–MF_5$ about the bridging fluorine) and the torsion angle ψ (twisting of the two planar $MF_{4,eq}$ groups from an eclipsed to a staggered conformation). In $K_3Cr_2F_{11}$·2HF, the bridging angle is 141°, and the dihedral angle is 43°. Because of the large bending of the Cr–F–Cr angle, the fluorine atoms are found in a staggered

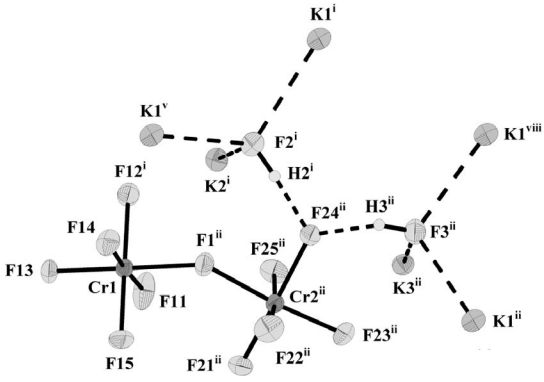

Figure 16. The $[Cr_2F_{11}]^{3-}$ dimer and K^+ cations with interacting HF molecules in $K_3Cr_2F_{11}$·2HF (thermal ellipsoids are drawn at the 50% probability level).

(*gauche*) conformation to minimize their repulsions. Deviation from the ideal D_{4h} symmetry is caused by hydrogen bonding and long interionic contacts in the solid state. In $[C_5H_6]_2[H_3O][Ti_2F_{11}]\cdot 2H_2O$, the dimeric $[Ti_2F_{11}]^{3-}$ anions are well separated by bulky organic cations, which results in linear almost symmetrical dimers ($\alpha = 180°$; ψ is close to zero).[28]

The Cr–F_t bonds are shorter (1.757–1.817 Å), as expected, than the Cr–F_b bonds involved in the Cr1–F1–Cr2 bridge [1.916(3) Å, 1.924(5) Å] or the Cr–F24 bonds involved in hydrogen bonding [1.901(5) Å] (Table 7). Two crystallographically nonequivalent HF molecules form hydrogen bonds with the same fluorine atom belonging to the $[Cr_2F_{11}]^{3-}$ dimer. The F2···F24 and F3···F24 distances (2.455 Å and 2.51 Å) are similar to the corresponding distances found in $A_2CrF_6\cdot 2HF$ (A = Na, K) and $Cs_2CrF_6\cdot 4HF$. Additionally, each HF molecule forms contacts with three different potassium cations.

Table 7. Selected Cr–F bond lengths [Å] in $K_3Cr_2F_{11}\cdot 2HF$.[a]

Cr1–F11	1.778(4)	Cr2–F22	1.757(4)
Cr1–F15	1.778(4)	Cr2–F25	1.771(4)
Cr1–F14	1.785(4)	Cr2–F23	1.777(3)
Cr1–F12^{i}	1.790(4)	Cr2–F21	1.788(5)
Cr1–F13	1.817(4)	Cr2–F24	1.901(5)
Cr1–F1^{ii}	1.924(5)	Cr2–F1	1.916(3)

[a] Symmetry codes: (i) $x + 1/2, -y + 3/2, z + 1/2$; (ii) $x + 1/2, -y + 1/2, z + 1/2$; (iii) $-x, -y + 1, -z + 1$; (iv) $-x + 1/2, y - 1/2, -z + 3/2$; (v) $-x + 1/2, y + 1/2, -z + 3/2$; (vi) $-x + 1, -y + 1, -z + 1$; (vii) $-x + 1/2, y + 1/2, -z + 1/2$; (viii) $x, y + 1, z$; (ix) $x, y - 1, z$; (x) $x - 1/2, -y + 3/2, z - 1/2$; (xi) $x - 1/2, -y + 1/2, z - 1/2$; (xii) $-x + 1/2, y - 1/2, -z + 1/2$; (viii) $1 - x, 1 - y, 2 - z$.

There are also three crystallographically nonequivalent K^+ cations in the crystal structure of $K_3Cr_2F_{11}\cdot 2HF$. The K–F bond lengths span a wide range (2.702–3.003 Å for K1, 2.683–2.978 Å for K2, and 2.652–3.054 Å for K3). The corresponding bond valences are 0.864 vu (K1), 0.967 vu (K2), and 1.127 vu (K3).

General Comments on Cr^{IV} Salts

In all the crystal structures considered, the F···F distances between the fluorine atoms involved in hydrogen bonding have very similar values ($Na_2CrF_6\cdot 2HF$: 2.469 Å; $K_2CrF_6\cdot 2HF$: 2.455 Å; $Cs_2CrF_6\cdot 4HF$: 2.466 Å; $K_3Cr_2F_{11}\cdot 2HF$: 2.455 Å and 2.51 Å). These values are slightly shorter than those in crystalline HF [2.49(1) Å][51] and considerably longer than the F···F distances in $[HF_2]^-$ anions (ca. 2.27 Å).[52,53] The FHF species in previously mentioned crystal structures are best described as HF molecules that are hydrogen-bonded to fluorine ligands of the $[CrF_6]$ octahedra. The F···(H)···F distances in the crystal structures reported herein are all in the range 2.5–3.2 Å. Hydrogen bonds falling in this range are classified as moderate-to-strong hydrogen bonds, which could be described as mostly electrostatic.[54]

For $K_3Cr_2F_{11}\cdot 2HF$, it could be argued that instead of a Cr^{4+} dimer, we have a mixed-oxidation state Cr^{3+}/Cr^{5+} dimer. Because of its thermal instability, no magnetic measurements were possible. Bond valence analysis[38–40,55] provides a powerful method to verify the formal oxidation states in crystal structures. Unfortunately, the bond valence parameter (R_{ij}) is not available for Cr^{4+} in the original article by Brese and O'Keeffe or by Brown and Altermart.[38–40] A value of 1.56 for R_{ij} has been proposed for Cr^{4+} in the latest reports.[56] The corresponding R_{ij} value for Cr^{3+} is 1.64[39]/1.657(5).[40] Since the bond valence parameters for bonds with fluorine do not depend strongly on the oxidation state,[39] the proposed value for Cr^{4+} seems too low. By using that value, an unreasonably low bond valence sum (2.944 vu) for Cr^{4+} in Li_2CrF_6 is obtained, while the use of R_{ij} determined for Cr^{3+} (1.64/1.657) gives better results (3.656/3.828 vu). For that reason, a new value of 1.6732 for R_{ij} was calculated from the crystal data of Li_2CrF_6 according to Brese and O'Keeffe's method.[39] The use of the universal constant $b = 0.37$ and of $R_{ij} = 1.6732$ gives reasonable bond valence sums for Cr in $Na_2CrF_6\cdot 2HF$ (4.078 vu), $K_2CrF_6\cdot 2HF$ (4.06 vu), $Cs_2CrF_6\cdot 4HF$ (4.078 vu), and $K_3Cr_2F_{11}\cdot 2HF$ (4.16 vu for Cr1 and 4.112 vu for Cr2). These values correspond to a +4 formal oxidation state of Cr.

Raman Spectra of $ACrF_6$ (A = K–Cs), A_2CrF_6 (A = Li–Cs), $A_2CrF_6\cdot 2HF$ (A = Na, K), $A_2CrF_6\cdot 4HF$ (A = Rb, Cs), $K_3Cr_2F_{11}\cdot 2HF$, and $ACrF_5$ (A = K–Cs)

Raman Spectra of the $[CrF_6]^-$ and $[CrF_6]^{2-}$ Salts

The Raman spectra of the $[CrF_6]^-$ and $[CrF_6]^{2-}$ salts are shown in Figures 17, 18, and 19, and additional details are given in Tables 8 and 9. The Raman spectrum of Cs_2CrF_6 is not presented. Irrespective of the synthetic approach, bands that could not be assigned to $[CrF_6]^{2-}$ were always observed in its spectrum. Since the Raman spectra of $K_2CrF_6\cdot 2HF$ and $A_2CrF_6\cdot 4HF$ (Rb, Cs) were recorded on single crystals covered with a thin layer of perfluorinated oil, assignment of the weak bands was problematic. Because of its volatility, the protecting layer of perfluorinated oil slowly disappears, and decomposition of the single crystals occurred. The most sensitive were the single crystals of

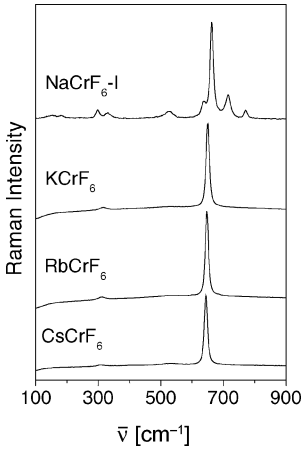

Figure 17. Raman spectra of $NaCrF_6$-I, $KCrF_6$, $RbCrF_6$, and $CsCrF_6$.

Cs_2CrF_6·4HF, and only the strongest two bands in the spectrum could be assigned unambiguously. The decomposition of Rb_2CrF_6·4HF to Rb_2CrF_6 was followed by Raman spectroscopy (Figure 19). After 30 min, in addition to the bands that can be assigned to Rb_2CrF_6 bands at ca. 1000 cm^{-1} appear. Rb_2CrF_6 is further hydrolyzed to the oxyfluoride species when it comes in contact with moisture from the atmosphere.

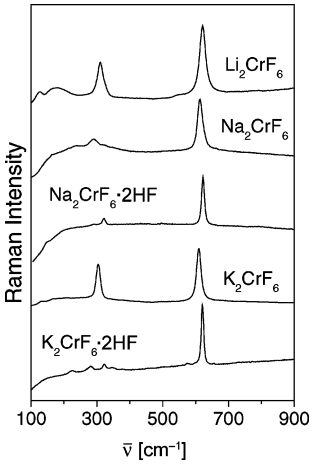

Figure 18. Raman spectra of the $[CrF_6]^{2-}$ salts of Li, Na, and K.

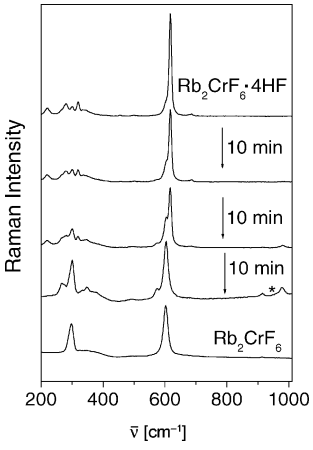

Figure 19. Raman spectra recorded in air during the decomposition of a single crystal of Rb_2CrF_6·4HF when the protective thin layer of oil slowly disappears. For comparison, the Raman spectrum of Rb_2CrF_6 is also given. The asterisk (*) denotes bands that could be assigned to oxyfluoride species.

Table 8. Raman spectra of $KCrF_6$, $RbCrF_6$, and $CsCrF_6$.[a]

$NaCrF_6$-I[b]	$KCrF_6$	$RbCrF_6$	$CsCrF_6$	Assignment[b]
771(6)				ν_3
715(15)				ν_3
662(100)	651(100)	647(100)	645(100)	ν_1
636(10)				ν_1
527(5)	533(vw)	537(<1)	533(<1)	ν_2
330(4)	315(5)	313(5)	308(5)	ν_5
299(6)				ν_5

[a] Intensities are given in parenthesis; vw = very weak. [b] Assignment is made for the octahedral symmetry, although in the solid state, the actual symmetry is lower.

The Raman spectra of the $[CrF_6]^-$ salts of K–Cs and $[CrF_6]^{2-}$ salts of Li–Cs are in agreement with those previously determined for $NOCrF_6$ and NF_4CrF_6 (average values: ν_1 = 649 cm^{-1}, ν_2 = 537 cm^{-1}, ν_5 = 308 cm^{-1}),[11] and $(NO)_2CrF_6$ (ν_1 = 608 cm^{-1}, ν_5 = 298 cm^{-1}),[11] respectively. As expected, the symmetrical stretching frequency (ν_1) increases as the oxidation state of the Cr atom increases. The ν_1 stretching modes for the compounds A_2CrF_6·*n*HF occur at higher frequencies relative to those for A_2CrF_6. This shift can be attributed to the moderate–to-strong hydrogen bonding between the $[CrF_6]^{2-}$ anions and the HF molecules. There is no satisfactory explanation for the very weak intensities of ν_2 ($[CrF_6]^-$ salts) or for the absence of ν_2 ($[CrF_6]^{2-}$ salts). In the Raman spectrum of $(NO)_2CrF_6$, the ν_2 mode was observed at 521 cm^{-1}.[11]

For the orthorhombic crystal modification of $NaCrF_6$, more vibrations are observed than those expected for regular $[CrF_6]$ octahedra with O_h symmetry. This is due to crystal field splitting as well as interactions between the cations and anions in the crystal lattice that lead to a strong distortion of the $[CrF_6]$ octahedra. In orthorhombic $NaCrF_6$ (space group *Pnma*, No. 62), the site symmetry of CrF_6 is C_s, but since Bravais cell contains four molecules of $NaCrF_6$, factor group splitting can further cause the degenerate modes to split into more components.[57–59] As a consequence of the lowering of the symmetry in the solid state (site symmetry and correlation effects) and the cation–anion interactions in the crystal lattice of $NaCrF_6$, vibrations which are otherwise Raman inactive in O_h symmetry become active (ν_3), and additionally, the splitting of the ν_1, ν_3, and ν_5 vibrations also occurs. The split ν_3 bands

Table 9. Raman spectra of the $[CrF_6]^{2-}$ salts.[a]

Li_2CrF_6	Na_2CrF_6	Na_2CrF_6·2HF	K_2CrF_6	K_2CrF_6·2HF	Rb_2CrF_6	Rb_2CrF_6·4HF	Cs_2CrF_6	Cs_2CrF_6·4HF	Assignment[b]
621(100)	613(100)	622(100)	609(100)	621(100)	603(100)	617(100)	600(100)	616(100)	ν_1
314(50)	322(sh.)	321(15)	304(60)	321(2)	298(60)	319(5)	295(60)	325(5)	ν_5
	293(20)			283(5)		280(4)			ν_5
				226(3)		220(2)			ν_5

[a] Intensities are given in parenthesis; sh. = shoulder. [b] Assignments are made for the octahedral symmetry, although in the solid state, the actual symmetry is lower.

occur at much higher frequencies (715 cm^{-1}, 771 cm^{-1}) relative to those found in $NOCrF_6$ (675 cm^{-1}) or NF_4CrF_6 (665 cm^{-1}).[11] Such a phenomenon is well described for the $[XF_6]^-$ (X = As, Sb) species. In the vibrational spectra of $CsAsF_6$[60] with regular $[AsF_6]^-$ octahedra, the Raman active symmetrical stretching (ν_1) mode occurs at 685 cm^{-1} and ν_5 at 372 cm^{-1}. The ν_3 mode is only infrared active (699 cm^{-1}). On the other hand, in the Raman spectrum of $[F_5TeNH_3][AsF_6]$[61] with highly distorted $[AsF_6]^-$ anions, ν_1 and ν_5 are split (ν_1 = 683 cm^{-1}, 689 cm^{-1}; ν_5 = 373 cm^{-1}, 377 cm^{-1}). Additionally, in $[F_5TeNH_3][AsF_6]$, nonactive ν_3 becomes Raman active, and is split and occurs at a higher frequency (716 cm^{-1}, 730 cm^{-1}, 740 cm^{-1}, 743 cm^{-1}) relative to ν_1 in $CsAsF_6$ (699 cm^{-1}).

$K_3Cr_2F_{11}$·2HF

In terms of the number and relative intensities of the vibrational bands, the Raman spectrum of $K_3Cr_2F_{11}$·2HF (Figure 20, Table 10) closely resembles to that of the $[M_2F_{11}]^-$ (M = Sb) anions found in KSb_2F_{11}[62] and $[Pd(CO)_4][Sb_2F_{11}]$.[63] In both compounds, the $[M_2F_{11}]^-$ anions strongly deviate from the ideal D_{4h} symmetry. Partial assignment of the $[Cr_2F_{11}]^{3-}$ anion was made on the basis of comparison of the Raman spectra. In KSb_2F_{11}, there are three crystallographically nonequivalent, highly distorted $[M_2F_{11}]^-$ anions with a bridge angle of 149.2°, 150.4°, and 146.1° and three corresponding dihedral angles of 20.2°, 21.2°, 32.6°, while in $[Pd(CO)_4][Sb_2F_{11}]$, there are two crystallographically nonequivalent $[M_2F_{11}]^-$ anions with a bridge angle of 151° and 159° and two corresponding dihedral angles of 9° and 38°. In $K_3Cr_2F_{11}$·2HF, the bridging M–F_b–M angle is 141° and the dihedral angle is 43°.

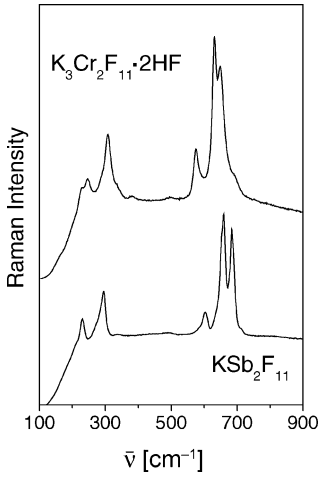

Figure 20. Raman spectra of $K_3Cr_2F_{11}$·2HF and KSb_2F_{11}.

The bands in the region 575–650 cm^{-1} and band at 695 cm^{-1} are assigned to Cr–F_{eq} (F_{eq} = equatorial fluorine atoms in *cis* to F_b) and Cr–F_{ax} (F_{ax} = axial fluorine atoms in *trans* to F_b) stretches, respectively, while the band around 500 cm^{-1} is typical of M–F–M bridging. Bands below 310 cm^{-1} are assigned to bending deformations.

Table 10. Vibrational spectrum of $K_3Cr_2F_{11}$·2HF and literature data of KSb_2F_{11}.[a],[b]

$K_3Cr_2F_{11}$·2HF	KSb_2F_{11}	Assignments[c]
695(sh.)	713(sh.)	$\nu(MF_{ax})$
650(80)	684(85)	$\nu(MF_{4eq})$
632(100)	660(100)	$\nu(MF_{4eq})$
575(31)	654(sh.)	$\nu(MF_{4eq})$
	603(20)	$\nu(MF_{4eq})$
498(1)		ν(MFM)
383(3)	339(5)	?
335(sh.)		
308(38)	295(40)	$\delta(MF_{4eq})$
288(sh.)	271(sh.)	$\delta(MF_{4eq})$
247(11)	231(15)	$\delta(MF_{4eq})$
230(8)		$\delta(MF_{4eq})$

[a] Ref.[62] [b] Intensities are given in parenthesis; sh. = shoulder. [c] ν = stretching mode, δ = deformation mode.

Raman spectra of $ACrF_5$ (A = K, Rb, Cs)

Reports on the vibrational spectra of compounds consisting of $[MF_5]_n^{n-}$ chains of anionic octahedra sharing joint vertices are scarce. For XeF_2·CrF_4 (*trans* sharing, Figure 6a), (XeF_5CrF_5)·XeF_4 (*cis–trans* sharing, Figure 6b), and XeF_5CrF_5 (*cis* sharing, Figure 6c) the simple approach was used.[64] Raman bands in the range 631–765 cm^{-1} are attributed to the stretching vibrations of the terminal fluorine atoms, and the bands in the range 502–544 cm^{-1} to stretching vibrations of the bridging fluorine atoms. The remaining bands (below 300 cm^{-1}) are assigned to bending and lattice vibrations. Structures with chains of anionic octahedra have been determined or proposed for various $[GeF_5]^-$ salts.[65,66] In their case a more sophisticated approach was used.[65] The normal modes of the germanium atom and the four nonbridging (terminal) fluorine atoms were considered separately from those of the germanium atom and the bridging fluorine atoms. The germanium atom and the four fluorine atoms form a group with D_{4h} (*trans* sharing in XeF_5GeF_5) or C_{2v} (*cis* sharing in ClO_2GeF_5, NO_2GeF_5, and SF_3GeF_5) symmetry.[65] The former has seven and the latter nine fundamental vibrations. Complete assignment was carried out only for XeF_5GeF_5 (D_{4h}, *trans* sharing).[65] In the case of the remaining compounds (*cis* sharing), only partial assignment was reported.[65]

The compounds $ACrF_5$ have complex Raman spectra (Table 11, Figure 21). The anion consists of infinite chains ($[CrF_5]_n^{n-}$) of $[CrF_6]$ octahedra that share *cis* vertices. In the crystal structure of $CsCrF_5$, the Cr–F–Cr bridges in the infinite chains $[CrF_5]_n^{n-}$ have an angle of 180°. In $RbCrF_5$, the corresponding Cr–F–Cr bridges are bent with an angle of 149.4°, which results in lower symmetry. As in the case of ClO_2GeF_5 (*cis* sharing), the most intense Raman band of the $ACrF_5$ compounds (ca. 682 cm^{-1}) is assigned to the in-phase symmetric stretch of the $[CrF_4]$ group (i.e. Cr–nonbridging-F stretching). The bands between 420 and 630 cm^{-1} may be assigned to the stretching modes of the

chain. The band in the region 360–380 cm^{-1} can tentatively result from the deformation angle between [CrF_4] group and the bridging fluorine atoms. The bands between 230 cm^{-1} and 340 cm^{-1} are attributed to deformations of the [CrF_4] group. The lower frequency bands (166–220 cm^{-1}) are in the range of torsional and rotational motions of the infinite chains and lattice vibrations.

Table 11. Raman spectra of $KCrF_5$, $RbCrF_5$, and $CsCrF_5$.[a]

$KCrF_5$	$RbCrF_5$	$CsCrF_5$	Assignment[b]
683(100)	682(100)	681(100)	ν_{Cr-Ft}
629(sh.)	622(sh.)		ν_{chains}
604(65)	599(67)	595(80)	ν_{chains}
		495(vw, br.)	ν_{chains}
		421(w, br.)	ν_{chains}
381(5)	363(4)		$\delta_{chain-CrF4}$
336(14)	335(10)	341(10)	δ_{CrF4}
314(sh.)	308(sh.)	319(7)	δ_{CrF4}
300(30)	298(27)	288(20)	δ_{CrF4}
253(25)	258(31)	261(46)	δ_{CrF4}
229(22)	226(18)	236(19)	δ_{CrF4}
		220(12)	τ_{chain}
208(sh.)	207(sh.)	208(sh.)	τ_{chain}, lattice vib.
188(2)	174(5)	166(9)	τ_{chain}, lattice vib.

[a] Intensities are given in parenthesis; vw = very weak, w = weak, br. = broad. [b] ν_{Cr-Ft} = Cr–nonbridging-F stretching vibrations, ν_{chains} = stretching vibrations of chains, $\delta_{chain-CrF4}$ = chain–CrF_4-group angle deformation, δ_{CrF4} = bending modes of the CrF_4 group, τ_{chain} = chain torsional rotational modes.

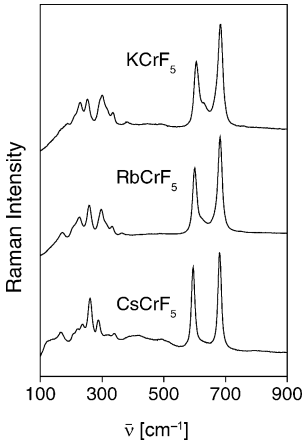

Figure 21. Raman spectra of $KCrF_5$, $RbCrF_5$, and $CsCrF_5$.

Summary and Conclusion

Photochemical synthesis and crystal structure determination of alkali metal hexafluorochromates(V) complete the void in the group of $A^IM^VF_6$ compounds;[29] more than 100 compounds have been reported. The thermal stability of the compounds decrease from the Li to Cs salt, which is in agreement with the decrease in the Lewis acidity (i.e. fluoride-ion donor properties increase from LiF to CsF). Polymorphism of $NaCrF_6$ has been found. The orthorhombic phase ($NaCrF_6$-I) has a marginally smaller molecular volume than the hexagonal phase ($NaCrF_6$-II), and it is probably the thermodynamically stable modification.

In contrast to previous expectations, the thermal decomposition of $CsCrF_6$ does not provide a simple route to monomeric CrF_5.[67] Instead, $CsCrF_6$ is reduced to $CsCrF_5$. The same happens with $RbCrF_6$. $LiCrF_6$ and $NaCrF_6$ release CrF_5 and fluorine, and are converted to A_2CrF_6. $KCrF_6$ lies at the border of the two cases. The thermal decomposition of $KCrF_6$ in a closed system leads to $KCrF_5$, while when CrF_5 is removed from the system, K_2CrF_6 is found as final product.

In the crystal structures of $ACrF_5$ (A = K, Rb, Cs), a new manner of forming infinite $[CrF_5]_n^{n-}$ chains of [CrF_6] octahedra joined through shared *cis* vertices was observed. The crystal structures determined are, with the exception of some Zr, Hf, and Tb compounds, the only examples of fully determined crystals structures of the $A^IM^{IV}F_5$ compounds. Attempted preparations of the corresponding Li and Na compounds were unsuccessful, most likely because of the small size of the Li^+ and Na^+ cations, which does not allow effective packing of the infinite $[CrF_5]^{n-}$ chains.

Single crystals of a new type of compound with the general formula $A^I_2M^{IV}F_6 \cdot nL$ (L = neutral ligand) were grown, and their crystal structures determined. In spite of the great number of reports on $A^I_2M^{IV}F_6$ type of compounds, we were not able to find any other data on such examples. This opens further questions: first, whether $A^I_2M^{IV}F_6 \cdot nHF$ complexes can be formed also by other M^{4+} transition metals, and second, whether, instead of HF, some other neutral ligand can be involved.

$[Cr_2F_{11}]^{3-}$ represents a rare example of a triply charged dimeric anion. Previously, only $[Ti_2F_{11}]^{3-}$ was known.[28] In contrast to the latter, $[Cr_2F_{11}]^{3-}$ is highly distorted in which the fluorine atoms are found in a staggered conformation.

Our study showed that the preparation of pure A_2CrF_6 compounds is still problematic. The reported syntheses involving the fluorination of mixtures of $ACl/CrCl_3$ with elemental fluorine at elevated temperatures[26,27] or mixtures of $ACl/CrCl_3$ with BrF_3[25] yield impure products. Our attempts to prepare pure A_2CrF_6 compounds by the annealing of $AF/ACrF_5$ mixtures at 473 K were partly successful. Although X-ray powder diffraction data corresponded only to the presence of A_2CrF_6 phases, starting materials or other species could be present as shown by Raman spectroscopy. The latter was found to be a very efficient tool for the qualitative indication of the purity of obtained products.

Experimental Section

Caution: Anhydrous HF, fluorine, and the fluorine-containing compounds should be handled only in a well-ventilated hood, and protective clothing should be worn all times!

Techniques: Raman spectra with a resolution of 1 cm^{-1} were recorded (10–20 scans) on a Renishaw Raman Imaging Microscope

System 1000, with the 632.8-nm exciting line of a He–Ne laser (50 mW). The $ACrF_6$ (A = Na–Cs) compounds decomposed in the laser beam. Because of this reason, the power was reduced to ca. 20%. X-ray powder diffraction patterns were obtained by using the Debye–Scherrer technique with Ni-filtered Cu-K_α radiation. Samples were loaded into quartz capillaries (0.3 mm) in a dry-box. Intensities were estimated visually. A 400-W medium pressure mercury lamp (Baird and Tatlock, London, Type 400 LQ) was used as the UV source.

Reagents and Apparatus: Volatile materials were manipulated by using an all PTFE vacuum line equipped with PTFE valves as previously described.[68] The manipulation of the nonvolatile solids was accomplished in a dry argon atmosphere within a dry-box (M. Braun, Germany). The residual water in the atmosphere within the dry-box never exceeded 2 ppm. All reactions were carried out in FEP (PolyDraack, Germany) reaction vessels (with a height of 300 mm, inner diameter of 15.5 mm, and outer diameter of 18.75 mm) equipped with PTFE valves[69] and PTFE-coated stirring bars. All reaction vessels were pretreated with F_2 prior to use. LiF (Merck, 99.9%), NaF (Merck, 99%), KF (Ventron, 99.9%), RbF (Aldrich, 99%), CsF (Ventron, 99.9%), CrF_3 (Messer Griesheim, 99.9%), and fluorine (Solvay) were used as supplied. BrF_3 was treated with elemental fluorine in order to remove possible traces of Br. CrF_5 was synthesized from CrF_3 under pressure of elemental fluorine.[70] CrF_4 was prepared by solvolysis of $XeF_2{\cdot}CrF_4$ in aHF.[16] Anhydrous HF (Fluka, Purum) was treated with K_2NiF_6 for several hours prior to use.

Reactions Between AF (A = Li, Na, K, Cs) and CrF_5 at 333 K: The reactions were carried out as described in the literature for the synthesis of $CsCrF_6$.[9] A sample of the alkali metal fluoride (AF, A = Na–Cs) was loaded into the FEP reaction vessel, and excess liquid CrF_5 was condensed onto the solid fluoride salt at 77 K. The reaction mixture was warmed up to 333 K. On the basis of their Raman spectra, it was concluded that the final products were mixtures of $ACrF_6/A_2CrF_6/ACrF_5$ (A = K, Rb, Cs), $ACrF_6/A_2CrF_6$ (A = Na), or A_2CrF_6 (A = Li). Some of the samples contained unidentified but most probably polymeric CrF_5 species.

Photochemical Synthesis of $ACrF_6$: In a dry-box, a sample of CrF_3 (3–5 mmol) and the corresponding amount of the fluoride AF (A = Li–Cs) were loaded into the FEP reaction vessel. Anhydrous HF (6–10 mL) was condensed onto the solid at 77 K, and the reaction mixture was brought to ambient temperature. Fluorine was slowly added at ambient temperature to a pressure of 3 bar in the reaction vessel. After 4–7 d, a new portion of fluorine was added. This was repeated many times such that the final excess of fluorine was approximately 2 to 3. When the pressure of fluorine added in one batch exceeded 3 bar, some of the reactions vessels were burnt through during the photochemical reactions. Such problems were never observed before during the photochemical synthesis of other binary and ternary fluorides.[30–34] The reaction mixtures were left to stir for 10–20 d at ambient temperature until clear, deep-red solutions were obtained. The volatiles were slowly pumped off over a few hours. Deep-red $ACrF_6$ (K, Rb, Cs) compounds could be isolated at ambient temperature. When these were dissolved in fresh aHF, deep-red clear solutions were obtained again. Deep-red $NaCrF_6$ was isolated at 243 K. When it is dry, it can be stored in a glove box at ambient temperature. When the volatiles were pumped away at ambient temperature, a mixture of $NaCrF_6$ and Na_2CrF_6 was obtained. Deep-red $LiCrF_6$ could be isolated at temperatures below 243 K. When aHF was condensed onto cold $LiCrF_6$ and the reaction vessel was brought to ambient temperature, a deep-red solution was obtained again. The isolation of $LiCrF_6$ was repeated at 243 K, and the dry sample was warmed to ambient temperature and left half an hour. Red-orange fumes of CrF_5 were observed. The sample was cooled in liquid nitrogen, and aHF was condensed onto the solid. When the reaction vessel was brought to ambient temperature, a red solid precipitated. The volatiles were pumped away at ambient temperature and caught in a nitrogen-cooled trap. The Raman spectrum showed bands that could be assigned to CrF_5. The Raman spectra of the $ACrF_6$ salts (A = Na–Cs) were recorded, and X-ray powder diffraction patterns were also recorded. Chemical analyses of the resulting isolated products are given in Table 15.

Thermal Decomposition of $ACrF_6$ (A = Li–Cs): A sample of $ACrF_6$ (150 mg) was placed in a nickel boat in a nickel reactor in a dry-box filled with argon. After the argon was pumped away, the valve on the metal reaction vessel was closed ("static vacuum"), and the sample was heated at 473 K. In some experiments, the valve was left open and the sample was pumped ("dynamic vacuum") during heating. Thermal decomposition of $ACrF_6$ (A = Rb, Cs) in a dynamic vacuum at 473 K yielded brick-red $ACrF_5$ compounds. Thermal decomposition of the Li and Na salts resulted in yellow-orange A_2CrF_6 compounds under the same conditions. The Raman spectrum of the product of the thermal decomposition of $NaCrF_6$ in a static vacuum showed only the presence of Na_2CrF_6. Thermal decomposition of $KCrF_6$ in a static vacuum gave brick-red $KCrF_5$, while in a dynamic vacuum, yellow-orange K_2CrF_6 was obtained. The Raman spectra of the isolated solids were recorded, X-ray powder diffraction patterns were also recorded, and chemical analyses were performed (Table 15).

Reactions Between AF (A = Na, K, Rb) and CrF_4 in BrF_3: Reactions were performed as previously described.[14] A mixture of CrF_4 (1–2 mmol) and the corresponding amount of AF (A = Na, K, Rb) was loaded into a reaction vessel in a glove-box. BrF_3 (4–5 mL) was condensed onto the reaction mixture, and the reaction vessel was brought to ambient temperature. In half an hour, a clear solution was obtained. Finally, the volatile materials were pumped off over several hours at 333 K. The Raman spectra and the X-ray powder diffraction patterns of the brick-red (K, Rb) and brownish–yellow (Na) isolated products showed that they consist of $ACrF_5$ (A = K, Rb) and Na_2CrF_6, respectively. Chemical analyses of $ACrF_5$ are given in Table 15.

Attempted Preparation of Pure A_2CrF_6 with BrF_3 (A = Na, K, Rb, Cs), by Flow Reaction (A = Cs) and by Annealing of AF and $ACrF_5$ (A = K, Rb, Cs) Mixtures: Reactions between 2ACl (or 2AF) and CrF_4 in BrF_3 were performed in a similar way as previously described for the synthesis of $ACrF_5$. Corn-sand colored solids were isolated. Although X-ray powder diffraction data of the products corresponded to the literature data, their Raman spectra showed additional bands that could not be assigned to the $[CrF_6]^{2-}$ salts.

Flow fluorination of a reaction mixture of 2CsCl (or 2CsF) and $CrCl_3$ (or CrF_3) at 673 K was carried out according to the method of Klemm and Huss.[26] The X-ray powder diffraction pattern corresponded to the cubic phase of Cs_2CrF_6;[27] however, the Raman spectrum showed bands that could not be assigned to $[CrF_6]^{2-}$.

Photochemical reactions between 2AF, CrF_3, and UV-irradiated F_2 in aHF yielded mixtures of $ACrF_6/A_2CrF_6$ as shown by Raman spectroscopy.

A_2CrF_6 (A = K, Rb, Cs) were prepared by the annealing of mixtures of AF and $ACrF_5$ at elevated temperature (473 K). The X-ray powder diffraction pattern of the isolated sand-yellow solids corresponded to the A_2CrF_6 phases. The Raman spectra of the K and Rb products showed only vibrational bands that could be as-

signed to $[CrF_6]^{2-}$, while the Raman spectrum of Cs_2CrF_6 showed the presence of starting $CsCrF_5$ and unidentifed species. K_2CrF_6 could be prepared also by the annealing of KF and $KCrF_6$ at 473 K in a static vacuum.

Solvolysis of $CsCrF_5$ in aHF: Powdered $CsCrF_5$ (ca. 1 mmol) was loaded into a double T-shaped apparatus. The reaction vessel was cooled to 77 K in liquid nitrogen, and aHF (8 mL) was condensed onto the sample. The reaction vessel was brought to ambient temperature. Precipitation of an amethyst-colored solid occurred. The liquid phase was rose-red. The reaction vessel was left for 0.5 h at ambient temperature, and the liquid phase then decanted off, and aHF condensed back onto the insoluble solid. After repeating this procedure several times, the volatile materials were pumped off at room temperature. The X-ray powder diffraction pattern and Raman spectra of the amethyst-colored isolated solid were in agreement with literature data for α-CrF_4.[13] The Raman spectrum of the brick-red solid isolated from the decanted solution was identical to that of a mixture of $CsCrF_5$ and CsF·*n*HF.

Attempted Preparation of KCr_2F_{11}, $K_3Cr_2F_{13}$, and $K_3Cr_2F_{11}$: An attempt to prepare KCr_2F_{11} was carried out in a manner similar to the photochemical synthesis of the $KCrF_6$ salts. The starting molar ratio n(KF):n(CrF_3) was 1:2. After several days, a deep-red clear solution was observed above the insoluble phase. The Raman spectrum of the isolated solid showed that it consists mainly of $KCrF_6$. The same procedure as that described above was repeated with a starting molar ratio n(KF):n(CrF_3) of 3:2. In 6 d, a clear solution formed. The Raman spectrum of the isolated solid showed that, instead of $K_3Cr_2F_{13}$, a mixture of $KCrF_6$ and K_2CrF_6 was obtained.

Mixtures of $3KF/2CrF_4$, $KF/2KCrF_6$, and $K_2CrF_6/KCrF_6$ were placed in a nickel boat in a nickel reactor in a dry-box. The samples were heated to 523–573 K. In the case of $KF/2KCrF_6$ and $K_2CrF_6/KCrF_6$, the autoclave was pumped during heating. Instead of $K_3Cr_2F_{11}$, only K_2CrF_6 was detected in all products by Raman spectroscopy and X-ray powder diffraction analysis.

Crystal Growth of $ACrF_6$ (A = K, Rb), $ACrF_5$ (A = K–Cs), Li_2CrF_6, A_2CrF_6·2HF (A = Na, K), A_2CrF_6·4HF (A = Rb, Cs), and $K_3Cr_2F_{11}$·2HF: In a general procedure, growth of the single crystals took place in a double T-shaped apparatus consisting of two FEP tubes (19 mm o.d. and 6 mm o.d.). The starting Cr compounds (100–300 mg of each) were loaded into the wider arm of the crystallization vessel in a dry-box. Anhydrous HF (approximately 4–8 mL) was then condensed onto the starting material at 77 K. The crystallization mixtures were brought to ambient temperature, and the clear solutions, which had developed, were decanted into the narrower arm. Some of the narrow arms were equipped with additional valves to allow separation from the wider part. Evaporation of the solvent from these solutions was carried out by maintaining a temperature gradient corresponding to about 10 K between both tubes for 1–2 weeks, and later by increasing this further to about 50 K for an additional month. The effect of this treatment was to enable aHF to slowly evaporate from the narrower tube into the wider tube, while leaving behind the crystals.

Deep-red single crystals of $ACrF_6$ were grown from clear deep-red solutions of $ACrF_6$. They could also be grown from mixtures of $ACrF_6/A_2CrF_6/ACrF_5$ (A = K–Cs) or $ACrF_6/A_2CrF_6$ (A = Na), partly dissolved in aHF, obtained by reaction between AF (A = Na–Cs) and CrF_5 at 333 K.

The $ACrF_5$ and A_2CrF_6 salts partly solvolyze in aHF to yield reddish (Na–Cs) or orange solutions (Li), respectively, and an amethyst-colored residue. After a few days, light-red single crystals of $ACrF_5$ (A = K, Rb, Cs) appeared in the decanted solution. Later, yellow crystals (K_2CrF_6·2HF, Rb_2CrF_6·4HF, Cs_2CrF_6·4HF) were grown. In the case of lithium, only orange single crystals of Li_2CrF_6 were obtained.

Crystallization of the $ACrF_6$ (A = K–Cs) salts resulted, quite often, in two or three different types of crystals in the same batch. They could be easily separated on the basis of their different colors, i.e. deep-red $ACrF_6$ (A = Na with hexagonal and orthorhombic phases in the same batch, K–Cs), light-red $ACrF_5$ (A = K–Cs), orange $K_3Cr_2F_{11}$·2HF, and yellow Na_2CrF_6·2HF, K_2CrF_6·2HF, Rb_2CrF_6·4HF, and Cs_2CrF_6·4HF. It seems that the $ACrF_6$ compounds were partly reduced by slow penetration of water through the walls of the reaction vessels, as already observed before in some other cases.[71]

The crystals were sometimes twinned or of very poor quality. Therefore, all crystallizations were repeated many times. Attempts to prepare suitable single crystals of $KCrF_5$, Rb_2CrF_6·4HF, and $CsCrF_6$ were only partly successful. The crystal structures of $KCrF_5$ and Rb_2CrF_6·4HF were determined with the use of the models for $RbCrF_5$ or Cs_2CrF_6·4HF, respectively, but the resulting data were not of satisfactory precision ($KCrF_5$: R_1 = 0.1209, wR_2 = 0.278; Rb_2CrF_6·4HF: R_1 = 0.1194, wR_2 = 0.2526). For those, only the unit cells are reported. Attempts to prepare single crystals of $CsCrF_6$ always resulted in a sticky material; the unit cell parameters were determined from powder data only.

The single crystals of $ACrF_6$ (A = Na–Cs), $ACrF_5$ (A = K–Cs), Li_2CrF_6, Na_2CrF_6·2HF, and $K_3Cr_2F_{11}$·2HF were stable at ambient temperature in an inert atmosphere. The crystallization products were immersed in a perfluorinated oil (ABCR, FO5960, melting point 263 K) in a dry-box. The single crystals were then selected from the crystallization products under the microscope (at temperatures between 265 and 273 K) outside the dry-box and then transferred into a cold nitrogen stream of the diffractometer.

The single crystals of K_2CrF_6·2HF, Rb_2CrF_6·4HF and Cs_2CrF_6·4HF were stable at ambient temperature only in the mother liquor. When the last traces of aHF were removed, the compounds began to release HF to yield yellow powders of the corresponding A_2CrF_6 compounds. These were isolated in a special way. When only a small amount of mother liquor was still visible (ca. 0.1 mL), the valve separating the wider and narrower arms was closed. The narrower arm containing the crystallization products was separated and cooled down to 263 K. Cold perfluorinated oil (approximately 1–2 mL) was added, the tube was cut, and a mixture of crystals and oil was transferred onto a cold glass plate under the microscope. Appropriate crystals were selected by maintaining the temperature between 265 and 275 K, and then transferred into a cold nitrogen stream of the diffractometer.

After diffraction measurements, all the crystals were checked by Raman spectroscopy. Additionally, selected thermally stable single crystals of $ACrF_6$ (A = Na–Cs), $ACrF_5$ (A = K–Cs), Li_2CrF_6, Na_2CrF_6·2HF, and $K_3Cr_2F_{11}$·2HF were placed inside 0.3-mm quartz capillaries in a dry-box, and their Raman spectra recorded.

Crystal Structure Determination: Data were collected on a Rigaku AFC7 diffractometer with Mercury CCD area detector by using graphite monochromated Mo-K_α radiation at 200 K. The data were corrected for Lorentz and polarization effects. A multiscan absorption correction was applied to all data sets. All structures were solved by direct methods by using the SIR-92[72] program and refined with SHELXL-97[73] software, implemented in program package WinGX.[74] For the structure of Na_2CrF_6·2HF, the positions of the hydrogen atoms were found in a difference Fourier map. For

Table 12. Summary of crystal data and refinement results for $ACrF_6$ (A = Na-I, Na-II, K, Rb).

	$NaCrF_6$-I	$NaCrF_6$-II	$KCrF_6$	$RbCrF_6$
Crystal system	orthorhombic	trigonal	trigonal	trigonal
Space group	*Pnma* (No. 62)	$R\bar{3}$ (No. 148)	$R\bar{3}$ (No. 148)	$R\bar{3}$ (No. 148)
a [Å]	9.3970(22)	5.224(5)	7.3315(8)	7.460(3)
b [Å]	5.8159(13)	5.224(5)	7.3315(8)	7.460(3)
c [Å]	7.7226(18)	14.013(12)	7.2148(10)	7.478(2)
V [Å^3]	422.06(16)	331.2(5)	335.85(7)	360.4(2)
Z	4	3	3	3
M_w [g mol^{-1}]	188.99	188.99	205.10	251.47
$\rho_{calcd.}$ [g cm^{-3}]	2.974	2.843	3.042	3.476
T [K]	200	200	200	200
μ [mm^{-1}]	2.848	2.723	3.519	12.478
R_1[a]	0.0268	0.0507	0.0480	0.0724
wR_2[b]	0.0691	0.1299	0.1017	0.1576
GOF[c]	1.191	1.281	1.034	1.088

[a] $R_1 = \Sigma||F_o| - |F_c||/\Sigma|F_o|$ for $I > 2\sigma(I)$. [b] $wR_2 = [\Sigma w(F_o^2 - F_c^2)^2/\Sigma w(F_o^2)^2]^{1/2}$ for $I > 2\sigma(I)$. [c] GOF = $[\Sigma w(F_o^2 - F_c^2)^2/(N_o - N_p)]^{1/2}$, where N_o = no. of reflections and N_p = no. of refined parameters.

Table 13. Summary of crystal data and refinement results for $ACrF_5$ (A = Rb, Cs).

	$KCrF_5$[a]	$RbCrF_5$	$CsCrF_5$
Crystal system	orthorhombic	orthorhombic	orthorhombic
Space group	–	$Pmc2_1$ (No. 26)	*Pnma* (No. 62)
a [Å]	5.425(2)	5.5150(17)	10.70(2)
b [Å]	7.427(2)	7.653(14)	5.611(8)
c [Å]	9.824(4)	10.181(5)	7.936(11)
V [Å^3]	395.8(2)	429.7(8)	476.5(14)
Z	–	4	4
M_w [g mol^{-1}]	186.1	232.47	279.91
$\rho_{calcd.}$ [g cm^{-3}]	–	3.593	3.902
T [K]	200	200	200
μ [mm^{-1}]	–	13.905	9.922
R_1[a]	–	0.0386	0.0397
wR_2[b]	–	0.0993	0.0742
GOF[c]	–	1.185	1.125

[a] Because of the poor quality of the crystals obtained and consequently the poor quality of the collected data, only lattice parameters are given. $R_1 = \Sigma||F_o| - |F_c||/\Sigma|F_o|$ for $I > 2\sigma(I)$. [b] $wR_2 = [\Sigma w(F_o^2 - F_c^2)^2/\Sigma w(F_o^2)^2]^{1/2}$ for $I > 2\sigma(I)$. [c] GOF = $[\Sigma w(F_o^2 - F_c^2)^2/(N_o - N_p)]^{1/2}$, where N_o = no. of reflections and N_p = no. of refined parameters.

the structures of $K_2CrF_6 \cdot 2HF$, $Cs_2CrF_6 \cdot 4HF$, and $K_3Cr_2F_{11} \cdot 2HF$, the positions of the hydrogen atoms were determined geometrically. By taking into account the *R* values of 0.024 and 0.136 for the $\bar{3}$ and $\bar{3}m1$ Laue symmetry (corresponding to $R\bar{3}$ and $R\bar{3}m$ space groups, respectively), the structure of $KCrF_6$ was solved and refined in the $R\bar{3}$ (No. 148) space group. The search for higher symmetry, realized by the ADDSYM procedure implemented in the PLATON program package,[75] resulted in the $R\bar{3}m$ (No. 166) space group. Refinements in the $R\bar{3}$ and $R\bar{3}m$ space groups led to R_1/wR_2 values of 0.0480/0.1017 and 0.0626/0.1338, respectively. The Hamilton test[76] unequivocally indicates that $R\bar{3}$ is the correct choice and found that the additional symmetry appears to be pseudo-symmetry. Large thermal displacement ellipsoids of the linearly bridging fluorine atoms in the crystal structure of $CsCrF_5$ suggested that the linearly bridging fluorine atom is not on the Cr–F–Cr axis but slightly off the axis. A consequence of this could be that the mirror plane running through Cr–F–Cr in $CsCrF_5$ is not real. This could be caused by the presence of twinning in the measured crystals. For this reason, the structure of $CsCrF_5$ was additionally refined in $Pna2_1$ space group, which has a lower symmetry than *Pnma*. The refinement in an acentric space group did not improve the results. The Cr–F–Cr angle appeared to be noticeably smaller than 180°, but problems with the shape of the thermal ellipsoids of the ter-

Table 14. Summary of crystal data and refinement results for Li_2CrF_6, $A_2CrF_6 \cdot 2HF$ (A = Na, K), $Cs_2CrF_6 \cdot 4HF$, and $K_3Cr_2F_{11} \cdot 2HF$.

	Li_2CrF_6	$Na_2CrF_6 \cdot 2HF$	$K_2CrF_6 \cdot 2HF$	$Rb_2CrF_6 \cdot 4HF$[a]	$Cs_2CrF_6 \cdot 4HF$	$K_3Cr_2F_{11} \cdot 2HF$
Crystal system	tetragonal	monoclinic	monoclinic	monoclinic	monoclinic	monoclinic
Space group	$P4_2/mnm$ (No. 136)	$C2/m$ (No. 12)	$P2_1/c$ (No. 14)	–	$P2_1/n$ (No. 14)	$P2_1/n$ (No. 14)
a [Å]	4.5777(4)	7.395(4)	5.235(3)	7.326(5)	7.579(6)	11.694(8)
b [Å]	4.5777(4)	7.947(4)	8.031(2)	6.861(5)	7.133(5)	7.541(4)
c [Å]	8.8649(10)	5.386(3)	8.473(7)	9.353(7)	9.813(8)	13.552(10)
β [°]	–	115.247(7)	92.178(9)	108.28(8)	107.911(9)	111.102(14)
V [Å^3]	185.77(3)	286.3(3)	356.0(4)	446.4(5)	504.8(7)	1114.9(13)
Z	2	2	2	–	2	4
M_w [g mol^{-1}]	179.88	252.00	284.22	452.96	511.85	470.32
$\rho_{calcd.}$ [g cm^{-3}]	3.216	2.923	2.651	–	3.368	2.802
T [K]	200	200	200	200	200	200
μ [mm^{-1}]	3.115	2.253	2.861	–	8.343	3.222
R_1[b]	0.0421	0.0301	0.0469	–	0.0689	0.0573
wR_2[c]	0.1109	0.0809	0.1104	–	0.1728	0.1436
GOF[d]	1.279	1.186	1.092	–	1.106	1.188

[a] Because of the poor quality of the crystals obtained and consequently the poor quality of the collected data, only lattice parameters are given. [b] $R_1 = \Sigma||F_o| - |F_c||/\Sigma|F_o|$ for $I > 2\sigma(I)$. [c] $wR_2 = [\Sigma w(F_o^2 - F_c^2)^2/\Sigma w(F_o^2)^2]^{1/2}$ for $I > 2\sigma(I)$. [d] GOF = $[\Sigma w(F_o^2 - F_c^2)^2/(N_o - N_p)]^{1/2}$, where N_o = no. of reflections and N_p = no. of refined parameters.

minal fluorine atoms appeared. Moreover, both the ADDSYM procedure (implemented in program package PLATON) and CheckCif procedure (on IUCR webpage) found additional pseudo-symmetry and recommended the space group *Pnma*. It appears that the low quality of the $CsCrF_5$ crystals is the main reason for the unsatisfactory shape of the thermal ellipsoids of the bridging fluorine atoms. Unfortunately, all attempts to prepare better quality crystals of this compound were unsuccessful. The figures were prepared using DIAMOND 3.1 software.[77] Crystal and structure refinement data are given in Tables 12, 13, and 14.

Further details of the crystal-structure investigation may be obtained from the Fachinformationszentrum Karlsruhe, 76344 Eggenstein-Leopoldshafen, Germany, on quoting the depository numbers: CSD-418670 ($NaCrF_6$-ort), -418671 ($NaCrF_6$-trig), -418672 ($KCrF_6$), -418673 ($RbCrF_6$), -418674 ($RbCrF_5$), -418675 ($CsCrF_5$), -418676 (Li_2CrF_6), -418677 (Na_2CrF_6·2HF), -418678 (K_2CrF_6·2HF), -418679 (Cs_2CrF_6·4HF), and -418680 ($K_3Cr_2F_{11}$·2HF).

Chemical Analyses: The sample was weighed in a dry-box and subsequently treated with water. The total fluoride content was determined after preceding decomposition of the sample by fusion with $KNaCO_3$ by direct potentiometry with a fluoride ion-selective electrode.[78] The chromium content was, in turn, determined by redox titration.[79] The results of the analyses of the isolated products are given in Table 15.

Table 15. Chemical analyses of Cr^{IV} and Cr^{V} ternary fluorides.

Product	Chemical analyses[a]				
	Calculated		Obtained		
	%Cr	%F	%Cr	%F	Molar ratio *n*(Cr):*n*(F)
$NaCrF_6$[b]	27.52	60.33	26.8	58.2	1:5.94
$KCrF_6$[b]	25.4	55.6	25.2	53.8	1:5.84
$RbCrF_6$[b]	20.68	45.32	20.1	43.2	1:5.88
$CsCrF_6$[b]	17.40	38.14	17.20	37.4	1:5.95
$KCrF_5$[c]	27.90	51.04	27.0	49.1	1:4.98
$KCrF_5$[d]	27.90	51.04	27.2	49.6	1:4.99
$RbCrF_5$[c]	22.36	40.86	21.0	39.6	1:5.16
$RbCrF_5$[e]	22.36	40.86	20.8	38.2	1:5.00
$CsCrF_5$[e]	18.57	33.94	18.3	33.3	1:4.98
Li_2CrF_6[f]	28.91	63.38	29.0	61.9	1:5.84
Na_2CrF_6[e]	24.53	53.78	24.7	52.0	1:5.76
K_2CrF_6[e]	21.29	46.68	20.5	45.0	1:6.00
Cs_2CrF_6[g]	12.04	26.40	11.6	24.5	1:5.78
Cs_2CrF_6[h]	12.04	26.40[c]	11.9	25.2	1:5.80

[a] The chemical analyses are given in mass percent. [b] Prepared by photochemical reactions. [c] Prepared in liquid BrF_3. [d] Prepared by thermal decomposition of $ACrF_6$ at 473 K in static vacuum. [e] Prepared by thermal decomposition of $ACrF_6$ at 473 K in dynamic vacuum. [f] Prepared by decomposition of $LiCrF_6$ at ambient temperature. [g] Prepared by the annealing of a $CsF/CsCrF_5$ mixture at 573 K. [h] Prepared by annealing of a $CsF/CsCrF_5$ mixture.

Supporting Information (see footnote on the first page of this article): Raman spectra of $ACrF_6$ (A = K, Rb, Cs), of the products of the reactions between AF (A = Li, Na; K, Cs) and CrF_5 at 333 K, of the products of the reactions between AF (A = Li, Na), CrF_3, and UV-irradiated F_2 in aHF isolated at 243 K and ambient temperature, of $ACrF_6$ (A = Li, Cs) dissolved in aHF, of solid $LiCrF_6$ recorded at about 233 K, of CrF_5 obtained by thermal decomposition of $LiCrF_6$, of K_2CrF_6 obtained by thermal decomposition of $KCrF_6$ in dynamic and static vacuum at 573 K, of $ACrF_5$ (A = K, Rb) obtained by reaction between AF and CrF_4 in BrF_3, of the product obtained by the reaction between NaF and CrF_4 in BrF_3, of the products obtained by reaction between 2AF (A = Na, K, Rb) and CrF_4 in BrF_3, of the product obtained by flow fluorination of 2CsCl and $CrCl_3$ at 673 K, of the product obtained by photochemical reaction between 2KF, CrF_3, and UV-irradiated F_2 in aHF, of the products obtained by the annealing of AF (A = K, Rb, Cs) and $ACrF_5$ at 473 K, of the product obtained by the annealing of KF and $KCrF_6$ in static vacuum 673 K, of the solid residue after solvolysis of $CsCrF_5$ in aHF, of the products obtained by the annealing of mixtures of $3KF/CrF_4$ and $K_2CrF_6/KCrF_6$ at elevated temperature, of the decomposition of $KCrF_6$ in a laser beam, and of a partly decomposed single crystal of Cs_2CrF_6·4HF, and X-ray powder data for $CsCrF_6$ are presented.

Acknowledgments

The authors gratefully acknowledge the Slovenian Research Agency (ARRS) for financial support of the present study within the research program: P1-0045 Inorganic Chemistry and Technology.

[1] F. A. Cotton, G. Wilkinson, C. A. Murillo, M Bochmann in *Advanced Inorganic Chemistry*, 6th. ed., John Wiley & Sons, New York, **1999**, pp. 749–750.
[2] J. D. Lee in *Concise Inorganic Chemistry*, 4th ed., Chapman & Hall, London, **1991**, pp. 721–722.
[3] N. N. Greenwood, A. Earnshaw in *Chemistry of the Elements*, Pergamon Press, **1984**, pp. 1193–1196.
[4] C. L. Rollinson, "The Chemistry of Chromium, Molybdenum and Tungsten" in *Comprehensive Inorganic Chemistry* (Eds.: J. C. Bailar Jr, H. J. Emeléus, R. Nyholm, A. F. Trotman-Dickenson), Pergamon Press, Oxford, **1973**, pp. 688–691.
[5] M. McHughes, R. D. Willett, H. B. Davis, G. L. Gard, *Inorg. Chem.* **1986**, *25*, 426–427.
[6] R. Colton, J. H. Canterfold in *Halides of the first Row Transition Metals*, Wiley Interscience, London, **1969**, pp. 166–211.
[7] P. J. Green, B. M. Johnson, T. M. Loehr, G. L. Gard, *Inorg. Chem.* **1982**, *21*, 3562–3565.
[8] W. V. Rochat, J. N. Gerlach, G. L. Gard, *Inorg. Chem.* **1970**, *9*, 998–1000.
[9] S. D. Brown, T. M. Loehr, G. L. Gard, *J. Fluorine Chem.* **1976**, *7*, 19–32.
[10] W. A. Sunder, A. L. Wayda, D. Distefano, W. E. Falconer, *J. Fluorine Chem.* **1979**, *14*, 299–325.
[11] R. Bougon, W. W. Wilson, K. O. Christe, *Inorg. Chem.* **1985**, *24*, 2286–2292.
[12] O. Krämer, B. G. Müller, *Z. Anorg. Allg. Chem.* **1995**, *621*, 1969–1972.
[13] P. Benkič, Z. Mazej, B. Žemva, *Angew. Chem. Int. Ed.* **2002**, *41*, 1398–1399.
[14] H. C. Clark, Y. N. Sadana, *Can. J. Chem.* **1964**, *42*, 50–56.
[15] B. Hoffman, R. Hoppe, *Z. Anorg. Allg. Chem.* **1979**, *458*, 151–162.
[16] K. Lutar, I. Leban, T. Ogrin, B. Žemva, *Eur. J. Solid State Inorg. Chem.* **1992**, *29*, 713–727.
[17] K. Lutar, H. Borrmann, B. Žemva, *Inorg. Chem.* **1998**, *37*, 3002–3006.
[18] D. Avignant, I. Mansouri, R. Chevalier, J. C. Cousseins, *J. Solid State Chem.* **1981**, *38*, 121–127.
[19] D. Avignant, M. El-Ghozzi, V. Gaumet, *Eur. J. Solid State Inorg. Chem.* **1997**, *34*, 283–293.
[20] D. Koller, B. G. Müller, *Z. Anorg. Allg. Chem.* **2002**, *628*, 575–579.
[21] M. El-Ghozzi, D. Avignant, *J. Fluorine Chem.* **2001**, *107*, 229–233.
[22] V. Gaumet, D. Avignant, *Acta Crystallogr., Sect. C* **1997**, *53*, 1176–1178.
[23] D. Babel, *Struct. Bonding (Berlin)* **1967**, *3*, 1–73.

[24] G. Siebert, R. Hoppe, *Z. Anorg. Allg. Chem.* **1972**, *391*, 113–116.
[25] D. H. Brown, K. R. Dixon, R. D. W. Kemmitt, D. W. A. Sharp, *J. Chem. Soc.* **1965**, 1559–1560.
[26] E. Huss, W. Klemm, *Z. Anorg. Allg. Chem.* **1950**, *262*, 25–32.
[27] H. Bode, E. Voss, *Z. Anorg. Allg. Chem.* **1956**, *286*, 136–141.
[28] L. Q. Tang, M. S. Dadachov, X. D. Zou, *Z. Kristallogr. New Cryst. Struct.* **2001**, *216*, 387–388.
[29] Z. Mazej, R. Hagiwara, *J. Fluorine Chem.* **2007**, *128*, 423–437.
[30] O. Graudejus, S. H. Elder, G. M. Lucier, C. Shen, N. Bartlett, *Inorg. Chem.* **1999**, *38*, 2503–2509.
[31] G. M. Lucier, J. M. Whalen, N. Bartlett, *J. Fluorine Chem.* **1998**, *89*, 101–104.
[32] J. M. Whalen, G. M. Lucier, L. Chacón, N. Bartlett, *J. Fluorine Chem.* **1998**, *88*, 107–110.
[33] Z. Mazej, *J. Fluorine Chem.* **2002**, *114*, 75–80.
[34] Z. Mazej, *J. Fluorine Chem.* **2002**, *118*, 127–129.
[35] K. O. Christe, W. W. Wilson, R. D. Wilson, *Inorg. Chem.* **1980**, *19*, 3254–3256.
[36] A. Boultif, D. Luoer, *J. Appl. Crystallogr.* **1991**, *24*, 987–993.
[37] D. Babel, A. Tressaud in *Inorganic Solid Fluorides, Chemistry and Physics* (Eds.: P. Hagenmuller), Academic Press Inc., Orlando, **1985**, pp. 97–102.
[38] I. D. Brown, *Chem. Soc. Rev.* **1978**, *7*, 359–376.
[39] N. E. Brese, M. O'Keefe, *Acta Crystallogr., Sect. B* **1991**, *47*, 192–197.
[40] I. D. Brown, D. Altermatt, *Acta Crystallogr., Sect. B* **1985**, *41*, 244–247.
[41] K. Seppelt, *Acc. Chem. Res.* **2003**, *36*, 147–153.
[42] J. L. Pascual, *J. Chem. Phys.* **1998**, *109*, 11129–11130.
[43] G. Benner, R. Hoppe, *J. Fluorine Chem.* **1990**, *48*, 219–227.
[44] B. Ahsen, M. Berkei, G. Henkel, H. Willner, F. Aubke, *J. Am. Chem. Soc.* **2002**, *124*, 8371–8379.
[45] J. F. Gaw, Y. Yamaguchi, M. A. Vincent, H. F. Schaefer, *J. Am. Chem. Soc.* **1984**, *106*, 3133–3138.
[46] R. C. Guedes, P. C. Couto, B. J. C. Cabral, *J. Chem. Phys.* **2003**, *118*, 1272–1281.
[47] A. Kovács, Z. Varga, *Coord. Chem. Rev.* **2006**, *250*, 710–727.
[48] R. C. Fay, *Coord. Chem. Rev.* **1982**, *45*, 41–66.
[49] J. P. Laval, A. Abaouz, *J. Solid State Chem.* **1992**, *100*, 90–100.
[50] A. Abaouz, A. Taoudi, J. P. Laval, *J. Solid State Chem.* **1997**, *130*, 277–283.
[51] M. Atoji, W. N. Lipscomb, *Acta Crystallogr.* **1954**, *7*, 173–175.
[52] M. Gerken, J. P. Mack, G. J. Schrobilgen, R. J. Suontamo, *J. Fluorine Chem.* **2004**, *125*, 1663–1670.
[53] S. I. Troyanov, I. V. Morozov, E. Kemmnitz, *Z. Anorg. Allg. Chem.* **2005**, *631*, 1651–1654.
[54] T. Steiner, *Angew. Chem. Int. Ed.* **2002**, *41*, 48–76.
[55] I. D. Brown in *The Chemical Bond in Inorganic Chemistry, The Bond Valence Model*, Oxford University Press, **2002**.
[56] http://www.ccp14.ac.uk/ccp/web-mirrors/i_d_brown/.
[57] W. G. Fateley, F. R. Dollish, N. T. McDevitt, F. F. Bentley in *Infrared and Raman Selection Rules for Molecular and Lattice Vibrations*, Wiley Interscience, New York, **1972**.
[58] G. Turrell in *Infrared and Raman Spectra of Crystals*, Academic Press, London and New York, **1972**.
[59] J. C. Decius, R. M. Hexter in *Molecular Vibrations in Crystals*, McGraw-Hill, New York, **1977**.
[60] G. M. Begun, A. C. Rutenberg, *Inorg. Chem.* **1967**, *12*, 2212–2216.
[61] B. Fir, J. M. Whalen, H. P. A. Mercier, D. A. Dixon, G. J. Schrobilgen, *Inorg. Chem.* **2006**, *45*, 1978–1996.
[62] P. Benkič, H. D. B. Jenkins, M. Ponikvar, Z. Mazej, *Eur. J. Inorg. Chem.* **2006**, 1084–1092.
[63] H. Wilner, M. Bodenbinder, R. Bröchler, G. Hwang, S. J. Rettig, J. Trotter, B. Ahsen, U. Westphal, V. Jonas, W. Thiel, F. Aubke, *J. Am. Chem. Soc.* **2001**, *123*, 588–602.
[64] S. Milićev, K. Lutar, B. Žemva, T. Ogrin, *J. Mol. Structure* **1994**, *323*, 1–6.
[65] T. E. Mallouk, B. Desbat, N. Bartlett, *Inorg. Chem.* **1984**, *23*, 3160–3166.
[66] K. O. Christe, R. D. Wilson, I. B. Goldberg, *Inorg. Chem.* **1976**, *15*, 1271–1274.
[67] E. G. Hope, P. J. Jones, J. W. Levason, J. S. Ogden, M. Tajik, J. W. Turff, *J. Chem. Soc., Dalton Trans.* **1985**, 1443–1449.
[68] Z. Mazej, P. Benkič, K. Lutar, B. Žemva, *J. FLuorine Chem.* **2001**, *112*, 173–183.
[69] PTFE valves were constructed and made at Jožef Stefan Institute in a similar way as shown in: T. A. O'Donnell, "The Chemistry of Fluorine" in *Comprehensive Inorganic Chemistry*, Pergamon Press, Oxford, **1973**, p. 1918.
[70] J. Slivnik, B. Žemva, *Z. Anorg. Allg. Chem.* **1971**, *385*, 137–.
[71] W. J. Casteel, A. D. Dixon Jr, N. LeBlond, P. E. Lock, H. P. A. Mercier, G. J. Schrobilgen, *Inorg. Chem.* **1999**, *38*, 2340–2358.
[72] A. Altomare, M. Cascarano, M. C. Giacovazzo, A. Guagliardi, *J. Appl. Cryst.* **1993**, *26*, 343–350.
[73] G. M. Scheldrick, *SHELXL-97*, University of Göttingen, Germany, **1997**.
[74] L. J. Farrugia, *WinGX*, **1999**.
[75] A. L. Spek, *J. Appl. Crystallogr.* **2003**, *36*, 7–13.
[76] W. C. Hamilton, *Acta Crystallogr.* **1965**, *18*, 502–510.
[77] *DIAMOND v3.1, Crystal Impact GbR*, Bonn, Germany, **2004**–**2005**.
[78] M. Ponikvar, B. Sedej, B. Pihlar, B. Žemva, *Anal. Chim. Acta* **2000**, *418*, 113–118.
[79] N. H. Furman in *Standard Methods of Chemical Analysis*, 6th ed. (vol. 1), D. Van Nostrand Company, Princeton, **1962**, pp. 366–367.

Received: October 17, 2007
Published Online: March 3, 2008

